PONTIFICIA UNIVERSIDAD CATÓLICA DEL PERÚ

FACULTAD DE CIENCIAS E INGENIERÍA

EXPLORATION OF NOVEL INHIBITORS OF *MYCOBACTERIUM TUBERCULOSIS* DIHYDROFOLATE REDUCTASE FOR TUBERCULOSIS TREATMENT

Trabajo de investigación para obtener el grado académico de Bachiller en Ciencias con mención en Química

AUTORA

Kelly Cristina Mollo Palomino

ASESORA:

Helena Maruenda Castillo

Lima, Enero, 2024

Informe de Similitud

Yo, Helena Maruenda Castillo, docente de la Facultad de Ciencias e Ingeniería de la Pontificia Universidad Católica del Perú, asesora del Trabajo de Investigación para Bachillerato titulado:

"Exploration of novel inhibitors of Mycobacterium tuberculosis dihydrofolate reductase for tuberculosis treatment"

de la autora Kelly Cristina Mollo Palomino, dejo constancia de lo siguiente:

El mencionado documento tiene un índice de puntuación de similitud de 21%. Así lo consigna el reporte de similitud emitido por el software Turnitin el 22/01/2024.

He revisado con detalle dicho reporte y el Trabajo de Investigación para Bachillerato, y no se advierte indicios de plagio.

Las citas a otros autores y sus respectivas referencias cumplen con las pautas académicas.

Lugar y fecha: 22 de enero 2024

Apellidos y nombres de la asesora: Maruenda Castillo, Helena	
DNI: 06405962	Firma
ORCID: 0000-0002-4714-156X	

Abstract

Tuberculosis is a lethal illness caused by *Mycobacterium tuberculosis*, considered, to date, the second global cause of death. Despite this fact, the treatment still relies on 40-year-old paradigms, and with the rise of resistant tuberculosis cases and complications due to HIV co-infection, the need for new anti-tuberculosis agents becomes urgent.

An attractive target to consider for designing new drugs to fight tuberculosis is the enzyme *Mycobacterium tuberculosis* dihydrofolate reductase (*Mtb*DHFR), key macromolecule in the folate pathway whose inhibition would arrest DNA synthesis in the bacteria and lead to its death.

This thesis explores the molecular scaffolds reported during the last decade as virtual and *in vitro* inhibitors of *Mtb*DHFR that could be used as leads for further development. Also, it covers the state of the art of *Mtb*DHFR, in comparison with its human counterpart and the strategies used in the discovery of the selected inhibitors.

Resumen

La tuberculosis, enfermedad letal causada por la bacteria *Mycobacterium tuberculosis*, es considerada a la fecha la segunda principal causa de muerte a nivel global. A pesar de ello, el tratamiento contra la tuberculosis todavía se basa en paradigmas propuestos hace más de 40 años, y, con el incremento en los casos de tuberculosis resistente a fármacos y las complicaciones debido a la infección simultánea con VIH, la necesidad de identificar nuevos agentes contra la tuberculosis es una realidad.

Un blanco terapéutico a considerar en esta lucha es la enzima dihidrofolato reductasa de *Mycobacterium tuberculosis* (*Mtb*DHFR), una macromolécula clave en el ciclo del folato cuya inhibición detendría la síntesis del ADN en la bacteria, llevándola a su muerte.

Esta tesis busca explorar los esqueletos moleculares de inhibidores de *Mtb*DHFR – virtuales e *in vitro* – reportados en la literatura durante la última década, los cuales podrían ser empleados como moléculas líderes para un posterior desarrollo. Además, en esta tesis se cubre el estado del arte de la *Mtb*DHFR, en comparación con su contraparte humana, y las estrategias usadas para el descubrimiento de los inhibidores aquí presentados.

To my parents for helping me pursue my academic goals. To my sisters for listening and keeping me company during my late-night/early morning work.

To my best friend and companion, thank you for anchoring me to reality, for the intellectual conversations and discussions, endless understanding, and always looking out for my well-being.

To my classmates, who gave me a sense of belonging, became my friends, and whose companionship was essential to withstand our overloaded schedules during our last year of school. I will be forever grateful.

To Dr. Helena Maruenda, thank you for your patience, invaluable insight, vast knowledge, and wisdom. Your guidance made this thesis possible.
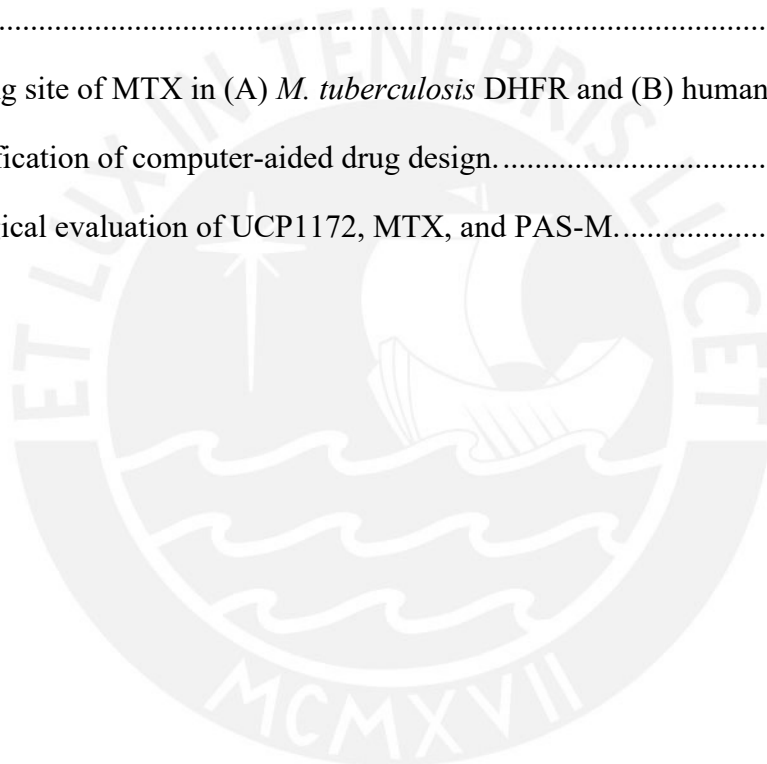
To Dr. Wilfredo Evangelista, who introduced me to the world of computational chemistry and helped me understand the new concepts in this area.

Table of contents

List of figures

List of tables

List of abbreviations

CADD   Computational-aided drug design

DHFR   Dihydrofolate reductase

DHF   Dihydrofolate

GOL   Glycerol

LBDD   Ligand-based drug design

MTX   Methotrexate

Mtb   *Mycobacterium tuberculosis*

NADPH   Nicotinamide adenine dinucleotide phosphate

QSAR   Quantitative structure-activity relationship

SHMT   Serine hydroxymethyltransferase

SBDD   Structure-based drug design

THF   Tetrahydrofolate

TB   Tuberculosis

XDR   Extensive drug resistant

1. Current outlook of tuberculosis

1.1. Demographics and mortality

Globally, tuberculosis (TB) is the leading cause of death from a single infectious agent: *Mycobacterium tuberculosis* (*Mtb*),[1] only second to SARS-CoV-2. However, due to the COVID-19 pandemia, a noticeable drop in the global number of newly diagnosed TB cases reported for the period 2019 - 2020, with a partial recovery in 2021 (Figure 1A), was observed.[2] This decrease suggests a larger number of undiagnosed and untreated TB cases in those years. The number of deaths, on the other hand, rose from 1.4 million in 2019 to 1.5 million in 2020 (Figure 1B) for HIV-negative people, reversing the global downtrend reported years before.[2] Given that deaths for TB in HIV-positive patients are officially considered under deaths due to HIV/AIDS, a distinction is required, as shown in figure 1B.
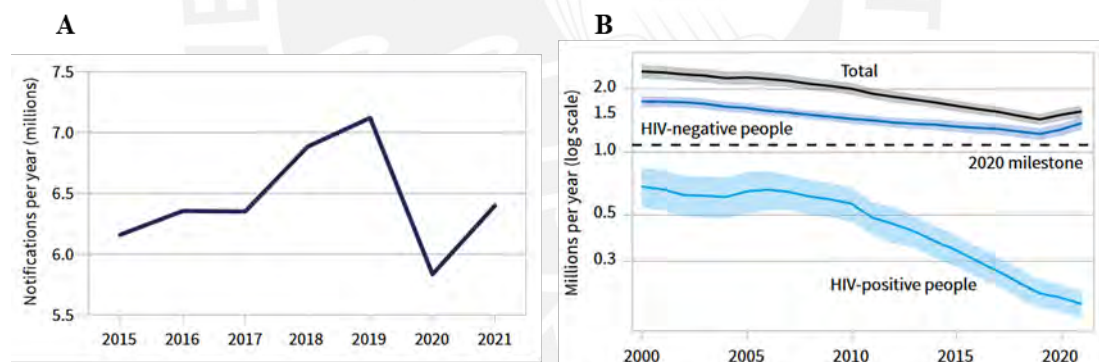
Figure 1. (A) Global trend in case notifications of newly diagnosed people with TB, 2015-2021. (B) Estimated number of TB deaths globally, 2000-2021. Shaded areas represent uncertainty intervals. Global tuberculosis report 2022. Geneva: World Health organization; 2022. Licence: CC BY-NC-SA 3.0 IGO.

Tuberculosis is not a new illness; its existence has been traced to the Stone Age Paleolithic period, 3.3 million years ago.[3] During the 18th and 19th centuries it became an epidemic in Europe and North America,[3] and, since 1882, the year that Robert Koch reported the causative agent behind TB, efforts were made to find a cure, finally achieved in the mid-20th century.[4] Although a decline in TB cases was observed in wealthier nations, this was not the case in the impoverished countries. The resurgence of TB in the US in 1980-1990s demonstrated that TB

was still a matter of concern. In 1993 the World Health Organization declared a "global health emergency".[4]

Despite its long history, scientists still struggle to find adequate treatments to fight the rising cases of resistant strains of TB and HIV co-infection, which cause the treatment to be longer, more expensive, and, sometimes, untreatable. In this scenario, the search for new inhibitors becomes of vital importance.

1.2. *Mycobacterium tuberculosis (Mtb)*

Mycobacterium tuberculosis (*Mtb*) is an aerobic pathogenic bacteria belonging to the family *Mycobacteriaceae*.[5] This pathogen has demonstrated to be resistant to various disinfectants such as alcohol (ethanol 70%), povidone iodine (1.0%), chlorhexidine gluconate (4%), quaternary ammonium compound (0.04% dimethyl benzylammonium chloride), and others,[6] chemical resistance that facilitates infection. Also, its complex cell envelope (Figure 2), formed by the interlinked layers of mycolic acids, arabinogalactan, and peptidoglycan, complicates treatment because it hinders the passage of hydrophilic molecules such as antibiotics.
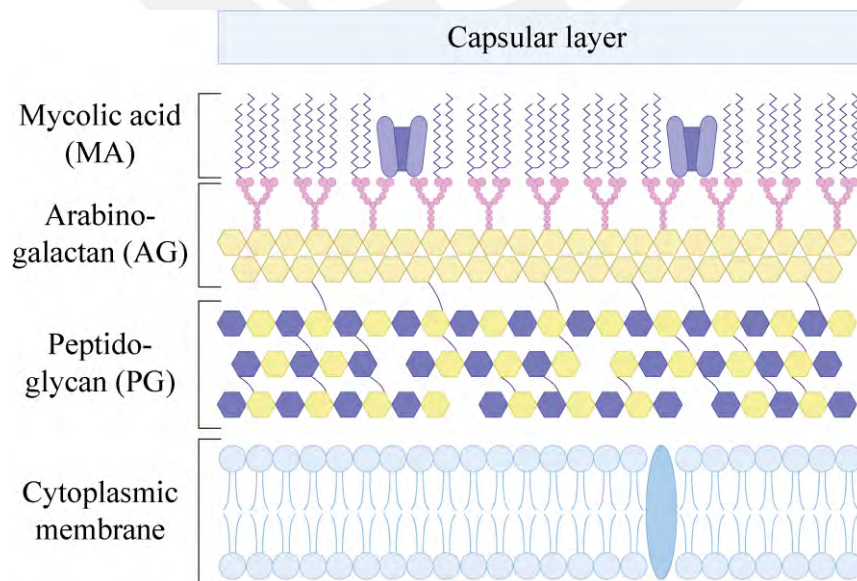

Figure 2. Structure of the cell envelope of *Mycobacterium tuberculosis*. Sketch based on references 7 and 8.

The outermost layer, mycolic acid (MA) layer, is made up of long-chain fatty acids comprised of α-alkyl-β-hydroxy chains, which account for the fluidity and permeability of the cell wall.[7] Also, the fluidity is thought to depend on how the cell wall lipids are organized, which is influenced by the mycolic acid structure, their length, and the presence of functional groups.[9] It has been proposed, that the hydrophobic nature of this layer is responsible for hindering the passage of small hydrophilic molecules like antibiotics.[10] When these molecules transverse the cell wall, it is believed that it is done by the passage through the water-filled pores –porins– present in the outer membrane.[9] The next layer is the arabinogalactan layer (AG in Figure 2), which is composed of a polysaccharide backbone that contains a single linear chain of thirty galactose units connected to three separate chains of thirty arabinose residues. This middle layer is covalently linked to the MA and the inner layer, peptidoglycan (PG). The innermost layer is composed of a polymer of sugar chains, cross-linked with short peptides. The sugar polymer is made of *N*-acetylglucosamine and *N*-acetylmuramic acid, which alternate and are displayed in a β configuration.[10]

1.2.1. Transmission of *Mtb*

Mycobacterium tuberculosis (*Mtb*) is spread from person-to-person through aerosol droplets. The size of these droplets determines the region of the respiratory airways they can reach. While smaller particles travel to the distal airways, larger ones could be trapped in the oropharynx leading to tuberculosis (TB) of cervical lymph nodes.[11]

Most of the droplets are expelled by the ciliated mucosal cells and only a small fraction is able to reach the lower respiratory tract.[12] Small aerosols carry small amounts of bacteria, yet, they are able to reach the alveolar spaces and are most likely to cause infection.[13] Once at the alveoli, the bacterium binds to the surface of alveolar macrophages and is phagocytized. The presence of *Mtb* reduces the acidity of the phagosome, inhibit the phagosome-lysosome fusion, and the

maturation of the phagosome.[12] Then, *Mtb* gathers macrophages onto the surface of the lungs and then macrophages transport the bacterium towards deeper tissues.[13] Afterwards, the infected cells drive immune cells towards them by triggering a local inflammatory response. This action results in the formation of granulomas, an organized ensemble of *Mtb*-infected and uninfected macrophages, whose membranes interlock like epithelial cells, and are at varying stages of maturation and differentiation.[13,14] The granuloma also contains neutrophils, dendritic cells, and fibroblasts circumscribed by T and B lymphocytes at its core, which becomes hypoxic with time, leading to necrosis at the core; this is termed the caseum.[14] Infected granuloma macrophages can die either by apoptosis or necrosis; when apoptosis takes place, it leaves the host cell membranes intact, thus confining the bacteria within the macrophage corpse. However, when necrosis takes place, the macrophages rupture, releasing the mycobacterium in a medium (necrotic debris of the granuloma or caseum) which supports its growth and multiplication. In addition, necrosis at the bronchial tree liberates mycobacteria through the airways in aerosolized droplets, thus ensuring the passage of the pathogen from one host to another.[13]

Although *M. tuberculosis* is usually associated with chronic lung disease, it can reside outside the lungs by entering the bloodstream and reaching various other organs, with lymph nodes being one of the most common sites.[15] This results in extrapulmonary TB, which can occur during the primary infection or years later through reactivation of TB.[12]

1.2.2. Resistance to treatment

The treatment for tuberculosis is usually long and complex, especially in those cases where resistance to the treatment has already emerged. The evolution of drug-resistant *M.* tuberculosis variants is partly attributed to inadequate control measures, noncompliance with the drug regimen, long term treatment, and inadequate prescription of drugs.[9,16] These actions lead to

structural changes in *Mtb*, such as mutations in genes that code for drug targets or for drug-activating enzymes.[17]

The mechanisms through which resistance occurs are either by the transmission of resistant strains to a new host or by developing drug resistance mutations to one or more drugs. These mutations hinder treatment greatly, with the level of drug resistance scaling from rifampicin resistant (RR) or isoniazid resistant (INH) to multidrug resistant (MDR) or extensive drug resistant (XDR). In the case of RR-TB or INH-TB, resistance is only towards rifampicin (RIF) or isoniazid (INH), respectively. Meanwhile, when infected with MDR-TB, resistance is to at least the two strongest anti-TB drugs, RIF and INH. Both RR- and MDR-TB have treatment periods longer than 18 months and require a combination of certain first- and second-line drugs.[16] Furthermore, the scenario is more discouraging when patients become infected with XDR-TB, because it is resistant to RIF and INH, but also to second-line drugs, fluoroquinolone, and at least one of the injectable drugs (capreomycin, kanamycin, and amikacin).

Finally, groups with weakened immune systems, such as patients with diabetes, cancer, organ transplant, and HIV/AIDS, are more likely to get infected with TB. One major problem is that HIV patients that acquire TB could experience drug-drug interactions. The HIV treatment requires life-long use of antiretroviral therapy and several MDR-TB agents inhibit major metabolic pathways of these antiretrovirals.[18]
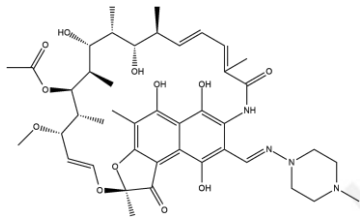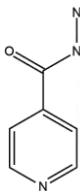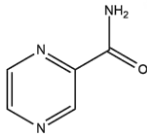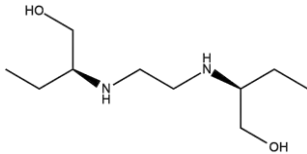
2. Chemotherapeutics

2.1. Typical chemotherapeutic targets against tuberculosis

Due to the varying degrees of resistance to treatment, the discovery and validation of new targets that could lead to drug-candidates is vital. These targets can be classified depending on the process of TB they intend to interrupt: DNA replication, protein synthesis, cell wall

biosynthesis, energy metabolism, and proteolysis of *M. tuberculosis*. In Tables 1 and 2, the targets of current inhibitors of first- and second-line drugs are reported, together with the drugs and their common adverse reactions.

Table 1. Specifications of first-line anti-TB agents.[a]

Drug name	Target protein	Common adverse reactions
Rifampicin (RIF)	β-subunit of RNA polymerase	Gastrointestinal reactions (nausea, vomiting, abdominal cramps, and diarrhea) and mild dermatological reactions (skin flush, itching, and/or rash).
Isoniazid (INH)	Catalase peroxidase NADH-specific enoyl-acyl carrier protein reductase β-ketoacyl ACP synthase	Peripheral neuropathy, hepatoxicity, cutaneous reaction (rash), jaundice, and fever.
Pyrazinamide (PZA)	30S ribosomal protein Aspartate decarboxylase Pyrazinamidase	Hepatoxicity, hyperuricemia with and without gout, fever, sideroblastic anemia, thrombocytopenia, lack of appetite, nausea, vomiting, dysuria, malaise, and it an also aggravate peptic ulcers.
Ethambutol (ETB)	Arabinosyltransferase Decaprenyl phosphate 5-phosphoribosyl synthase	Visual disturbances (diminished visual acuity, retrobulbar neuritis, retinal pigment displacement) and gastrointestinal symptoms (abdominal pain or vomiting).

[a] Information about targets extracted from reference 19 and adverse reactions from reference 20. Rifampicin adverse reaction was obtained from reference 21.

Table 2. Specifications of second-line anti-TB agents.
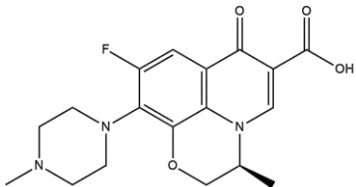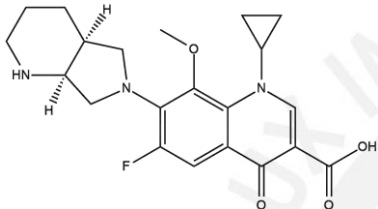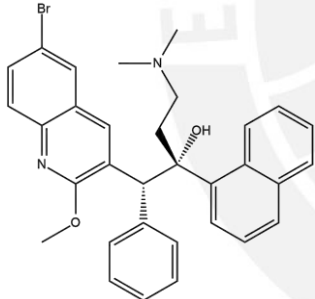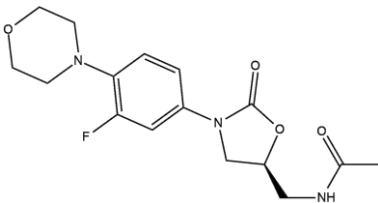
Drug name	Target protein	Common adverse reactions	Ref.
Group A			
Levofloxacin (Lfx)	DNA topoisomerase II and IV	Nausea, anxiety, headache, rash, abdominal pain, diarrhea, dizziness, and vomiting.	20,22
Moxifloxacin (Mfx)	DNA topoisomerase II and IV	QT interval prolongation and mild to moderate gastrointestinal disturbances (nausea, diarrhea).	20,22
Bedaquiline (Bdq)	ATP synthase subunit C Transcriptional repressor of Mmpl5	Nausea, arthralgia, headache, hemoptysis, chest pain, anorexia, and rash. It also affects the cardiovascular system by QT prolongation and it can elevate hepatic transaminases.	19,23
Linezolid (Lzd)	23S rRNA 50S ribosomal protein L3	Peripheral and optic neuropathy, anemia/thrombocytopenia, rash, and diarrhea.	19,24

Table 2 (continued).
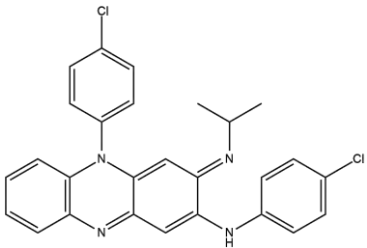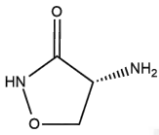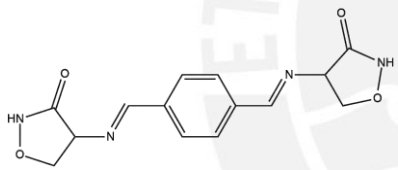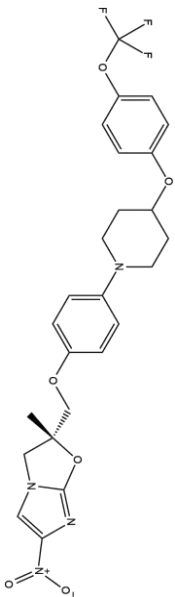
Group B			
Clofazimine (Cfz)	Mechanism of action is not fully understood. The mycobacterial respiratory chain and ion transporters are thought to be putative targets.	Abdominal/epigastric pain, nausea, diarrhea, vomiting, and gastrointestinal intolerance. It can cause ichthyosis, discoloration of the skin and conjunctiva, but its reversible.	25,26
Cycloserine (Cs)	Alanine racemase	Neurological disturbances (headache, somnolescence and tremors) and psychiatric disturbances (altered mood, cognitive deterioration, dysarthria, confusion, and even psychotic crises).	19,20
Terizidone (Trd)	L-alanine racemase D-alanine ligase	Seizures, dizziness, slurred speech, tremors, insomnia, confusion, depression, and suicidal tendency.	22
Group C[a]			
Delamanid (Dlm)	Deazaflavin (co-factor F_{420}) dependent nitroreductase	QTc interval prolongation.	19,22

Table 2 (continued).
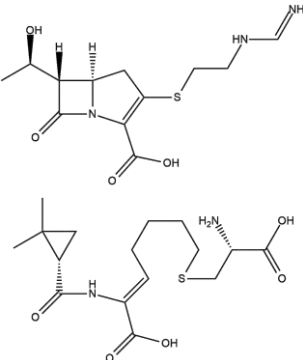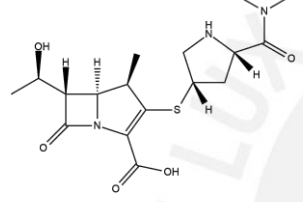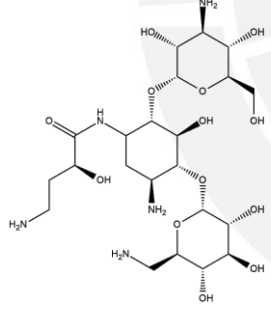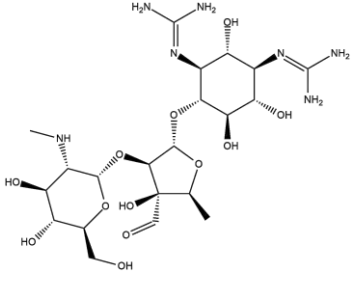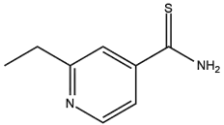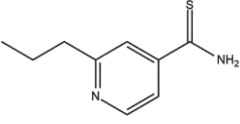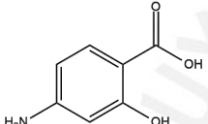
Imipenem–cilastatin (Ipm–Cln)	Penicillin-binding proteins (cilastatin does not have antibacterial activity, but it prevents degradation of imipenem and the protect kidneys against toxic effects)	Thrombophlebitis, nausea, diarrhea, and vomiting.	27
Meropenem (Mpm)	Penicillin-binding proteins	Diarrhea, nausea, vomiting, and rash.	28,29
Amikacin (Am)	16S rRNA	Ototoxicity or hearing impairment. Nephrotoxicity.	22,30, 31
Streptomycin (S)	16S rRNA protein S12	Nephrotoxicity and ototoxicity. Vertigo, ataxia, deafness, tinnitus, and cutaneous hypersensitivity.	22,32, 33

Table 2 (continued).

Ethionamide (Eto)	NADH-dependent enoyl-acyl carrier protein reductase	Gastrointestinal intolerance (nausea, vomiting, and lack of appetite). Risk of hepatitis.	20,22, 34
Prothionamide (Pto)	NADH-dependent enoyl-acyl carrier protein reductase	Gastrointestinal intolerance but lesser than Eto (nausea, vomiting, and lack of appetite). Risk of hepatitis. Menstrual disturbances.	20,22, 35
p-aminosalicylic acid (PAS)	Thymidylate synthase Dihydrofolate reductase	Drug-induced hepatitis, gastrointestinal intolerance, cutaneous hypersensitivity, and hypokalemia.	19,22, 33

[a] Group C also includes ethambutol (ETB) and pyrazinamide (PZA) (see Table 1).

2.2. Current treatment options and their limitations

The treatment for tuberculosis depends on the level of resistance of TB, with anti-TB agents currently being divided into first-line (Table 1) and second-line drugs (Table 2). The formulation of treatment is based upon past medical or social history, together with the local prevalence of resistance.[16] Therefore, the review of current anti-TB agents, according to the level of resistance and the understanding their side effects, is important to highlight the limitations of the current lines of treatment.

Within the first-line drugs are rifampicin (RIF), isoniazid (INH), pyrazinamide (PZA), and ethambutol (ETB) (Table 1). RIF is the cornerstone of TB treatment and, together with INH, PZA, and ETB are prescribed for cases of drug-sensitive TB, in patients who had no TB prior treatment in a 6-9 months regimen (intensive phase for 2 months).[16,36] The cure rate is 90-95% in TB control programs and trial conditions, yet patients might not tolerate the regimen.[36] When

using only RIF, patients might develop nausea, vomiting, diarrhea, loss of appetite, and hepatotoxicity.[37] Meanwhile, in combination therapy, the risk of developing drug-induced liver injury is greater than in the case of monotherapy.[38] A disadvantage of these side effects is that it leads to treatment interruption and contributes to drug resistance.

Once resistance has been developed, in cases such as RR-, INH-, MDR-, and XDR-TB, second-line drugs have to be used in combination with first-line agents, and are classified into groups A, B and C (Table 2).[39] In terms of length of treatment, WHO has elaborated guidelines according to the level of resistance.[40]

One of the issues with second-line agents is the severe adverse drug reactions (ADRs), with several concerning side effects including ototoxicity and psychosis-like symptoms.[41] These have led to the suspension of treatment in 19 to 60% of patients with MDR-TB. Among the targets included in Tables 1 and 2, dihydrofolate reductase (DHFR) highlights because its inhibitor, *p*-aminosalicylic acid (PAS), is the only antifolate currently on use; in particular for drug-resistant TB therapy.[42]

3. Dihydrofolate reductase *Mtb* as a chemotherapeutic target

3.1. Function, structure and active site of *Mtb*DHFR

Folate comprises co-factors that include three moieties: *p*-aminobenzoic acid (*p*ABA), pterin, and glutamate (Figure 3A).[43,44] While eukaryotes obtain this product from their diets, prokaryotes can *de novo* synthesize it. The biosynthesis begins with the formation of the pterin ring, followed by five reactions that lead to dihydrofolate (DHF), which is further reduced to tetrahydrofolate (THF) by DHFR (Figure 3).

DHFR is an enzyme from the oxidoreductases family that plays an essential role in the biosynthesis of tetrahydrofolate co-factors.[45] It catalyzes the reduction of DHF to THF,

11

employing nicotinamide adenine dinucleotide phosphate (NADPH) as co-factor (Figure 3A). Then, serine is converted into glycine by donating one carbon unit to THF at nitrogen-5 and nitrogen-10, resulting in the N^5,N^{10}-methylene-THF (mTHF) product (Figure 3B).[46] This reaction is reversible and it is catalyzed by the enzyme serine hydroxymethyltransferase (SHMT).[46,47] The products of the folate metabolism are thymidine, purines and methionine (Figure 3B).[47] Hence, the inhibition of DHFR leads to the interruption of DNA synthesis, and, this causes cell death.

Even though, *Mtb*DHFR seems like an attractive target for exploring new inhibitors of the folate pathway, since it is present in humans, *h*DHFR, the structural differences between both enzymes are important when addressing selectivity, in an effort to diminish toxicity. This has been the work of Li and collaborators, who found that regardless the difference in size between *h*DHFR (187 amino acids) and *Mtb*DHFR (159 amino acids), the protein folding of both of them is quite similar, as all DHFRs include a fold with a central *β*-sheet and four *α*-helices.[48] These enzymes, overall, only have a 26% amino acid sequence similarity, yet, at the active and ligand sites the similarity is higher (55%).[48]
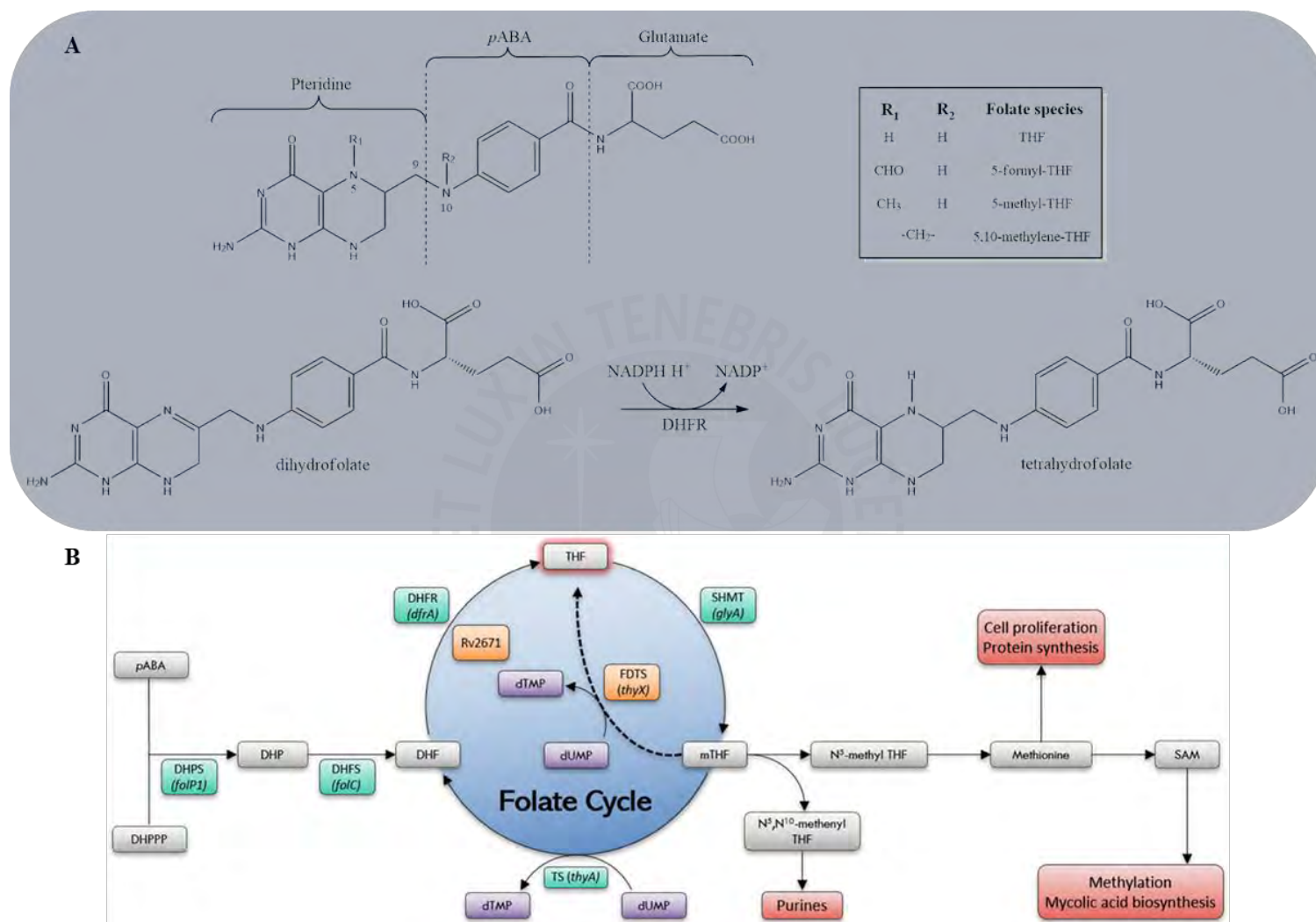
Figure 3. (A) Chemical moieties of folate and reduction of dihydrofolate to tetrahydrofolate by DHFR. (B) *Mycobacterium tuberculosis* folate pathway. The canonical enzyme pathway is given in green. The alternative pathway appears in orange. Figure 3B, reprinted from Cell Chemical Biology, 26, Hajian, B.; Scocchera, E.; Shoen, C.; Krucinska, J.; Viswanathan, K.; G-Dayanandan, N.; Erlandsen, H.; Estrada, A.; Mikušová, K.; Korduláková, J.; Cynamon, M.; Wright, D., Drugging the Folate Pathway in Mycobacterium Tuberculosis: The Role of Multi-Targeting Agents, 781-791, Copyright 2023, with permission from Elsevier.

To understand the active site of *Mtb*DHFR, and how it changes upon binding to its co-factor, substrate, and the inhibitor methotrexate (MTX), the 3D Protein Feature View on the RCSB Protein Data Bank website[49–51] (https://www.rcsb.org/) was used, in conjunction with the articles where the crystal structures of these complexes were first introduced. The crystal structures of *Mtb*DHFR in binary complex with NADPH (PDB: 1DG8) and in ternary complex with NADPH and inhibitor MTX (PDB: 1DF7) were both obtained by Li and collaborators[48]; in the case of the ternary complex with co-factor NADPH and substrate DHF (PDB: 6NND), this was reported by Ribeiro and collaborators[52]. The analysis of these studies has allowed to depict all the amino acid (aa) residues of *Mtb*DHFR that interact with NADPH, DHF, and MTX in these three *Mtb*DHFR complexes, here summarized in Table 3.
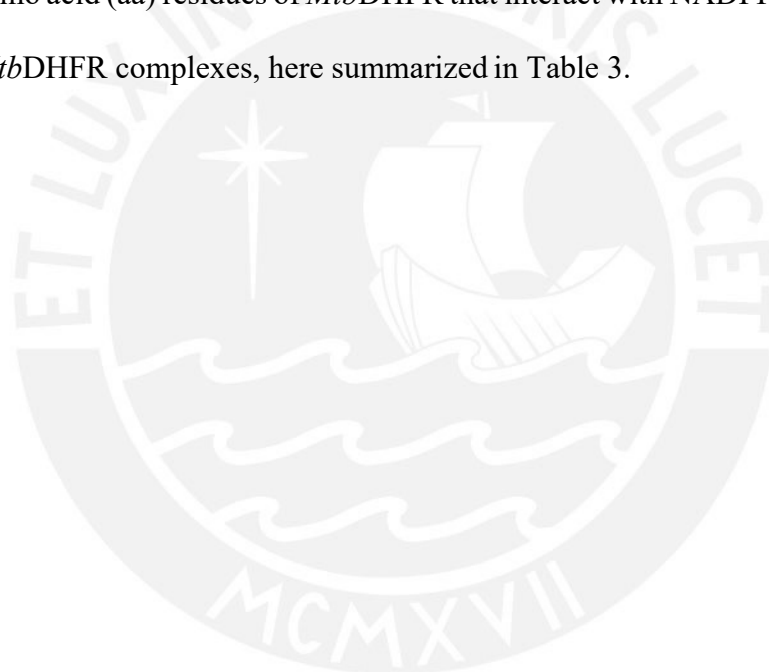
Table 3. List of amino acids that constitute the binding sites of NADPH, DHF, and MTX in *Mtb*DHFR.

Complex type	Binary	Ternary		Ternary		
Complexed w/	**NADPH**	**NADPH and DHF**		**NADPH and MTX**		
PBD	1DG8	6NND		1DF7		
Ref.	48,50	49,52		48,51		
	NADPH	**NADPH**	**DHF**	**NADPH**	**MTX**	**GOL**
	Trp6	**Trp6**	**Trp6**	Trp6	Ile5	Trp22
	Ala7	**Ala7**	**Ala7**	Ala7	Trp6	Leu24
	Ile14	Ile14	Asp27	Ile14	Ala7 [b]	Asp27
	Gly18	Gly15	Gln28	Gly15	Ile20	Gln28
	Asp19	Arg16	Ala29	Gly18	Pro25	
	Ile20 [a]	Gly18	Phe31	Asp19	Asp27	
	Gly43	Asp19	Arg32	Ile20	Gln28	
	Arg44	Ile20	Leu50	Gly43	Ala29	
	Arg45	Gly43	Val54	Arg44	Phe31	
	Thr46	Arg44	Leu57	Arg45	Arg32	
	Leu65	Arg45	Arg60	Thr46	Glu33 [c]	
	Ser66	Thr46	**Ile94**	Leu65	Ile50 [d]	
	Arg67	Leu65	Thr113	Ser66	Pro51	
	Gln68	Ser66		Arg67	Ile54 [d]	
	Gly80	Arg67		Gly80	Ile57 [d]	
	Ile94	Gly80		Ile94	Arg60	
	Gly96	**Ile94**		Gly96	Ile94	
	Gly97	Gly96		Gly97	Tyr100	
	Gln98	Gly97		Gln98		
	Val99	Gln98		Val99		
	Tyr100	Val99		Tyr100		
	Leu102	Tyr100		Leu102		
		Leu102		Ala126		

These residues are not included in the 3D Protein Feature View of the:

[a] 1DG8 PDB file, but it is reported as hydrophobic residue that approaches the nicotinamide ring in the study reported Li et al.

[b] 1DF7 PDB file, but specifically mentioned to form van der Waals interactions in the study reported Li et al.

[c] 1DF7 PDB file, but has been mentioned to provide a hydrophobic environment to MTX in the study reported Li et al.

[d] 1DF7 PDB file, but has been mentioned to be a negatively charged residue on the α-B helix, near the glutamate moiety of MTX, in the study reported Li et al. In the 1DF7 PDB file, residues Ile50, Ile54, Ile57 have reported as being Leu50, Val54, Leu57, respectively.

In order to better allocate these interactions, in Figure 4A and 4B, representations of the NADPH and DHF active sites obtained from the structural information available for *Mtb*DHFR in binary complex with NADPH and in ternary complex with NADPH and DHF, are shown. The structure of *Mtb*DHFR is composed of two main domains, both shown in Figure 4: the adenosine and the loop domain (Figure 4B), with the active site located in a groove, in between these domains.[52]
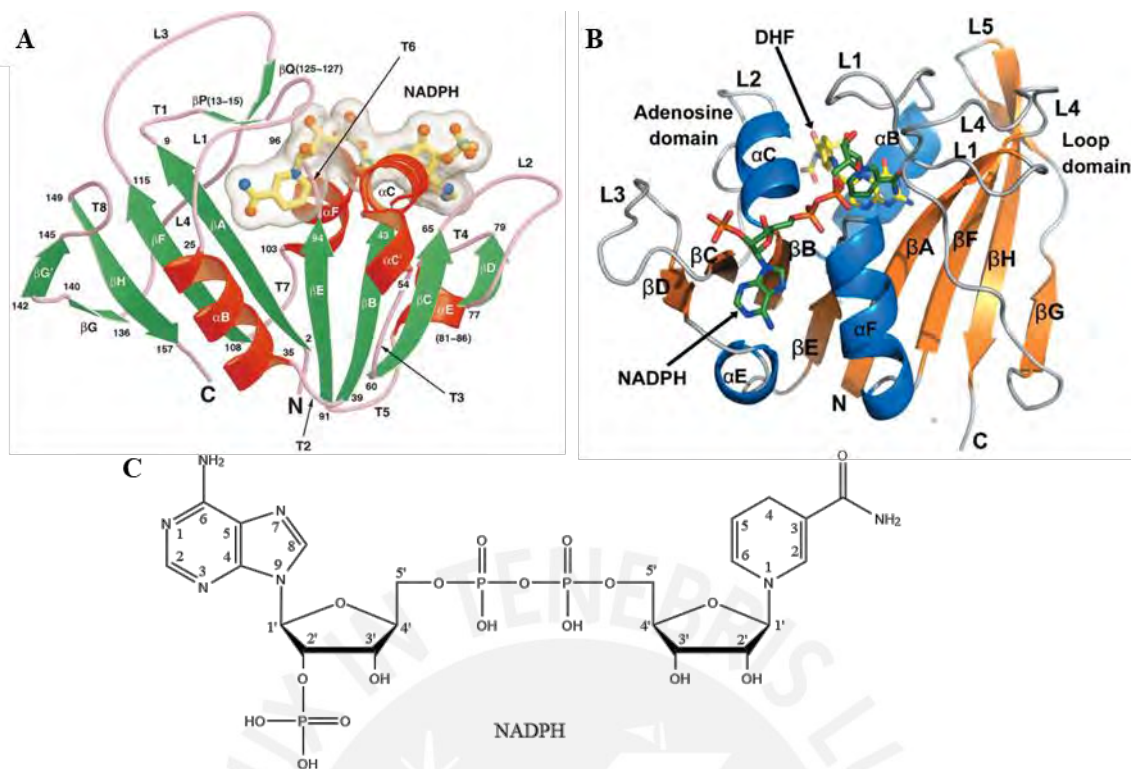
Figure 4. The structure of *Mtb*DHFR (A) in binary complex with co-factor NADPH and (B) in ternary complex with substrate DHF (in yellow), which binds to the adenosine domain, and co-factor NADPH (in green). (C) Chemical structure of co-factor NADPH. Figure 4A, reprinted from Journal of Molecular Biology, 295, Li, R.; Sirawaraporn, R.; Chitnumsub, P.; Sirawaraporn, W.; Wooden, J.; Athappilly, F.; Turley, S.; Hol, W. G., Three-Dimensional Structure of M. Tuberculosis Dihydrofolate Reductase Reveals Opportunities for the Design of Novel Tuberculosis Drugs, 307–323, Copyright 2023, with permission from Elsevier. Figure 4B, reprinted with permission from Ribeiro, J. A.; Chavez-Pacheco, S. M.; de Oliveira, G. S.; Silva, C. S.; Giudice, J. H. P.; Libreros-Zúñiga, G. A.; Dias, M. V. B. Crystal Structures of the Closed Form of Mycobacterium Tuberculosis Dihydrofolate Reductase in Complex with Dihydrofolate and Antifolates. *Acta Crystallogr. Sect. Struct. Biol.* **2019**, *75* (7), 682–693. https://doi.org/10.1107/S205979831900901X. Copyright 2023, with permission of the International Union of Crystallography.

Initially, upon entering the enzyme, NADPH (Figure 4C) buries into it, with the nicotinamide ring inserted into a crevice formed by strands β–A and β–F (Figure 4A). The residues Arg45 and Gln98 interact with the pyrophosphate moiety; Arg45 establishes a salt bridge while the side chain of Gln98 hydrogen bonds with the moiety. Meanwhile, adenine comes into contact with residues Ser66, Gly80, and Gln98, and it also interacts with residues to either side of its plane through hydrophobic interactions with residues Leu65 and Leu102, and through stacking interactions with the side chain of Arg67. The O2'-phosphate of NADPH establishes five hydrogen bonds with side chains of residues Ser66, Gln68, and Arg44 and the main-chain of Arg67. Also, the amide group of the nicotinamide ring forms three hydrogen bonds with

16

residues Ala7 and Ile14. In addition, residues Ile14 and Ile20 approach the nicotinamide ring from opposite sides.

In the case of the active site of NADPH in the ternary complex with DHF, from Table 3, almost all the residues that bind NADPH in the binary complex are retained. In addition, it is expected that for catalysis, NADPH needs to be in close contact with the pterin ring of DHF. This closeness is clear from Figure 4B and it is possible through interactions of both molecules – co-factor and substrate – with residues Trp6, Ala7, and Ile94 (in bold, Table 3). In the case of Ala7, for example, this residue hydrogen bonds with the nicotinamide moiety of NADPH, placing it over the DHF active site.[48] However, some differences are observed in the co-factor binding site, upon DHF binding to the apoenzyme: loss of interaction with residues Gln68 (which hydrogen bonded with pyrophosphate and was in contact with the adenine ring) on the ternary complex; and new interactions of NADPH with residues Gly15 and Arg16, only present in this ternary complex. Overall, it appears, as expected, that minimum changes occur in the co-factor site when the substrate binds to the enzyme.

To further describe the active site of *Mtb*DHFR, Ribeiro and collaborators, distinguished four sub-regions within the active site of *Mtb*DHFR:NADPH (Figure 5A).[53] Region (1) is the entry to the active site and it is positively charged, while region (2) is the central region of the active site and it is slightly apolar. Next, region (3) is negatively charged, and it is placed where the heteroaromatic ring of DHF accommodates. The region (4) is the site known as glycerol (GOL) binding site. The latter is known to accommodate a molecule of glycerol and it is relatively small; it is close in space to the DHF binding site and it is usually treated as an extension of it; this region is of hydrophilic nature.

Methotrexate is a clinically approved antifolate and an inhibitor of the *Mtb*DHFR enzyme, however, it is inactive in *Mtb* cultures.[54,55] It will be used as reference to observe the behavior

of the active site in presence of a inhibitor. As shown in Table 3, residues at the binding site of NADPH of *Mtb*DHFR in ternary complex with NADPH and MTX differ in two residues with respect to that of the complex with NADPH and DHF: the interaction between NADPH and residue Arg16 was lost, while a new one was established with Ala126. Similar to what was observed before, in ternary complex with DHF, the binding of MTX does not alter the interactions of NAPDH with the protein residues of *Mtb*DHFR.

However, the binding of MTX, when compared with DHF, is quite different. It is constituted by 18 aa instead of 13 (Table 3). The description of the interactions depicted by Li and collaborators[48] is illustrated in Figure 5. Residues Ile5, Ile94, and Tyr100 interact with the 4-amino group of MTX: the first two aa hydrogen bond with the 4-amino group while the latter, at 3.2 Å distance is now unable to stablish a hydrogen bond interaction.[48] Next, residue Asp27 hydrogen bonds both with the 2-amino group and the N1 of the inhibitor. The p-aminobenzoyl ring of MTX sits over the hydrophobic space created by these six residues: Ile50, Pro51, Ile54, Gln28, and Phe31. Also, the aminopterin ring of MTX is in contact with Trp6, Ala7, and Ile20 on one side, and with Phe31, Ile5, Ile94, and Gln28 on the other. The glutamate motif of MTX interacts with residues Gln28, Ala29, and Arg32 (in a loose manner), with hydrophobic residues Pro25 and Ala29, and with the negatively charged Glu33. Finally, the α-carboxyl group of this motif stablishes a salt bridge with positively charged residues Arg32 and Arg60. When contrasting the residues in Table 3, 7 out of 13 residues that describe the active site (DHF) interact with MTX. This explains well why MTX acts *in vitro* as a competitive inhibitor of the substrate.[56]
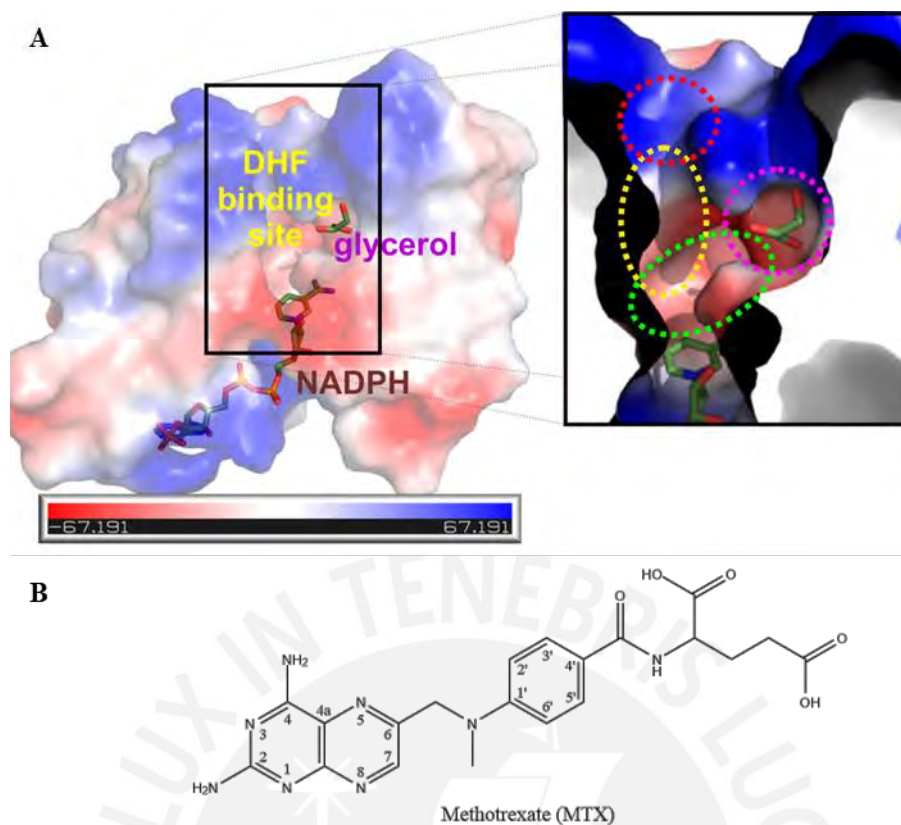
Figure 5. (A) Active site and sub-regions of *Mtb*DHFR. The inset has been divided in four regions: [1] positively charged region which bind to glutamate moiety of DHF, red; [2] central region of active site and *p*ABA sits, yellow; [3] dipyrimidine ring of DHF is stacked with nicotinamide moiety of NADPH, green; [4] glycerol-binding site, magenta. (B) Chemical structure of inhibitor MTX. Figure 5A, reprinted with permission from Ribeiro, J. A.; Hammer, A.; Libreros-Zúñiga, G. A.; Chavez-Pacheco, S. M.; Tyrakis, P.; de Oliveira, G. S.; Kirkman, T.; El Bakali, J.; Rocco, S. A.; Sforça, M. L.; Parise-Filho, R.; Coyne, A. G.; Blundell, T. L.; Abell, C.; Dias, M. V. B. Using a Fragment-Based Approach to Identify Alternative Chemical Scaffolds Targeting Dihydrofolate Reductase from Mycobacterium Tuberculosis. *ACS Infect. Dis.* **2020**, *6* (8), 2192–2201. https://doi.org/10.1021/acsinfecdis.0c00263. Copyright 2023 American Chemical Society.

As mentioned before, structural differences between *Mtb*DHFR and *h*DHFR are important for selectivity. The structure of *Mtb*DHFR bound to NADPH and MTX (PDB: 1DF7) shows the presence of a co-crystallized molecule of glycerol (GOL), which is absent in *h*DHFR (PDB: 1OHJ) (Figure 6A and B). GOL is bonded to *Mtb*DHFR through three hydrogen bonds to residues Asp27, Gln28, and Leu24.[48] In addition, GOL also interacts with the side chains of amino acids Trp22, Asp27, and Gln28 which form a hydrophilic pocket in *Mtb*DHFR.[48] In detail, the interactions with GOL, as described by El-Hamamsy and collaborators[57], are as follows: O(1)–H of GOL hydrogen bonds with the side-chain oxygen of Asp27 and O(1) of GOL hydrogen bonds with indole N–H of Trp22. Next, O(2) is an acceptor in the hydrogen bond with N-H of Gln28. Meanwhile, O(3)-H participates as a donor in a hydrogen bond with

19

the carbonyl of Leu24 and O(3) as an acceptor with N-H of Leu24. The lack of affinity of *h*DHFR for GOL may be explained by the fact that these amino acids – Trp22, Asp27, and Gln28 – are replaced by the hydrophobic residues Leu22, Pro26, and Gln28 in the human counterpart.[48] This difference is important when selecting *Mtb*DHFR inhibitors,[48,58] and therefore, should be better exploited.
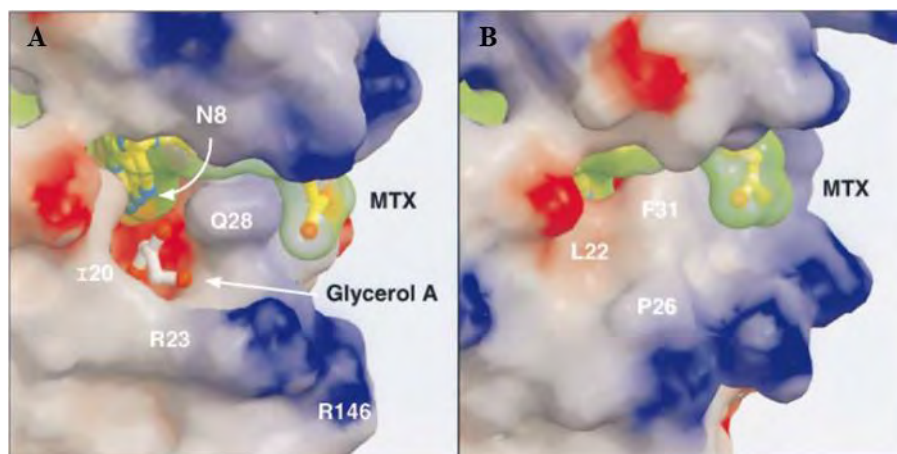
Figure 6. Binding site of MTX in (A) *M. tuberculosis* DHFR and (B) human DHFR. The glycerol A pocket is absent in *h*DHFR. Reprinted from Journal of Molecular Biology, 295, Li, R.; Sirawaraporn, R.; Chitnumsub, P.; Sirawaraporn, W.; Wooden, J.; Athappilly, F.; Turley, S.; Hol, W. G., Three-Dimensional Structure of M. Tuberculosis Dihydrofolate Reductase Reveals Opportunities for the Design of Novel Tuberculosis Drugs, 307–323, Copyright 2023, with permission from Elsevier.

In addition, Sharma and collaborators also compared both DHFR enzymes by *in silico* studies using PDB structures 1DF7 and 1OHJ for *Mtb*DHFR and *h*DHFR, respectively.[59] A π-stacking interaction was observed in this study between MTX and amino acid Phe31 in the *Mtb*DHFR active site.[59] However, this interaction was not validated by its crystal structure data. Instead, a cation-π interaction between Phe31 and the aminopterin ring of MTX could be observed when visualizing the 3D Protein Feature View of PDB 1DF7 on the RCSB Protein Data Bank website.[51]

Finally, it is relevant to add that there is an alternate folate pathway that uses enzyme Rv2671 (in orange, Figure 3B), the second DHFR found in *M. tuberculosis*.[60] This alternative way to reduce DHF induces resistance to antifolates and, therefore, multitarget inhibitors for both

*Mtb*DHFR and Rv2671 gain importance, as studied by Hajian and collaborators.[42] This is an aspect to keep in mind in future drug-design strategies.

3.2. Computational tools in search of *Mtb*DHFR inhibitors

Traditionally, drug design revolved around searching for active leads in culture broths or in biological extracts, that could later, once isolated and characterized, be developed into a potential drug.[61,62] Before the rise of target-based discovery, phenotype-based screening was the foundation of drug discovery. For this purpose, molecules were tested in cellular cultures or whole organisms such as zebrafish or *C. elegans*.[63] This method had the advantage of being able to discover "first-in-class" drug moieties,[63,64] but is time consuming as large compound libraries (0.4–2 million compounds) have to experimentally be tested.[65] Since the 70s, drug discovery has been predominantly accomplished by rational drug discovery, where the search is guided by a defined chemotherapeutical target.[62] The advantage of this approach is that inhibitors could further be structurally improved, searching for better pharmacological properties and lower toxicity values,[61,66] based on the structural data of the interaction with the target. This possibility makes it ideal for the refinement and development of more efficient drugs.

From conception to commercialization, drug development is expensive, with a cost of USD $1.6 billion,[67] and time consuming, usually 10 to 15 years.[66] This process involves several phases which includes: target identification, hit discovery, lead optimization, pre-clinical trials, clinical trials, approval, and post-approval.[66,68] Yet, despite the large investments made, there is high probability of failure at any stage of the process, with an attrition rate of drug candidates of 96%.[69] Therefore, strategies that could reduce the time of drug development and lower the costs, such as, computer-aided drug design (CADD),[68,70] are sought. CADD refers to the set of computational techniques that are used to identify and develop drugs by simulating drug–

receptor interactions.[70,71] Through these techniques, it is possible to identify target proteins, screen chemical libraries to identify potential drug candidates, and optimize these candidates.[69] In addition, the pharmacokinetics of the candidates can be predicted.[68] In this manner, it is possible to remove toxic compounds from the set of drug candidates, reducing the number of compounds to be evaluated experimentally.[69]

Computer-aided drug design can be roughly classified into two main categories, as shown in Figure 7: structure-based drug design (SBDD) and ligand-based drug design (LBDD). SBDD requires highly accurate structural data of the targets proteins,[68] which can be obtained experimentally from X-ray crystallography, cryo-electron microscopy, and nuclear magnetic resonance (NMR).[72] The structural information is important because it allows to estimate the binding affinity between ligands and the target macromolecule and allows to learn about the architecture of the binding site of the target protein,[69] as well as designing targe-specific compounds.[71]

In the cases were experimental structures are not available, 3D structure of target proteins can be developed through *in silico* prediction methods such as homology modelling or *ab* initio modelling.[69] Homology modelling, considered a prediction method of the highest degree of accuracy,[70] is based on the premise that proteins with highly conserved sequences will possess similar 3D structural conformations and functions.[69] Therefore, it is possible to deduce the 3D structure of a protein from its amino acid sequence by using a structural template protein with a similar sequence.[70] However, if protein templates are not available, it is possible to build 3D models, starting from the protein sequence, with *ab initio* modelling. For this purpose, the protein sequence undergoes a conformational search for the most thermodynamically stable conformations.[73] Still, these predictions are limited to small proteins (<120 residues).[73]

On the other hand, ligand-based drug design is used when the experimental 3D structure of the target protein is unavailable and a high-quality structure could not be attained through *in silico* prediction methods.[69] On the other hand, this approach relies on the knowledge of molecules that interact with a selected target[74] and on the principle that structural and physicochemical similarities would likely result in similar properties.[75] As a result, new drugs can be predicted based on active compounds for a certain target.[69]
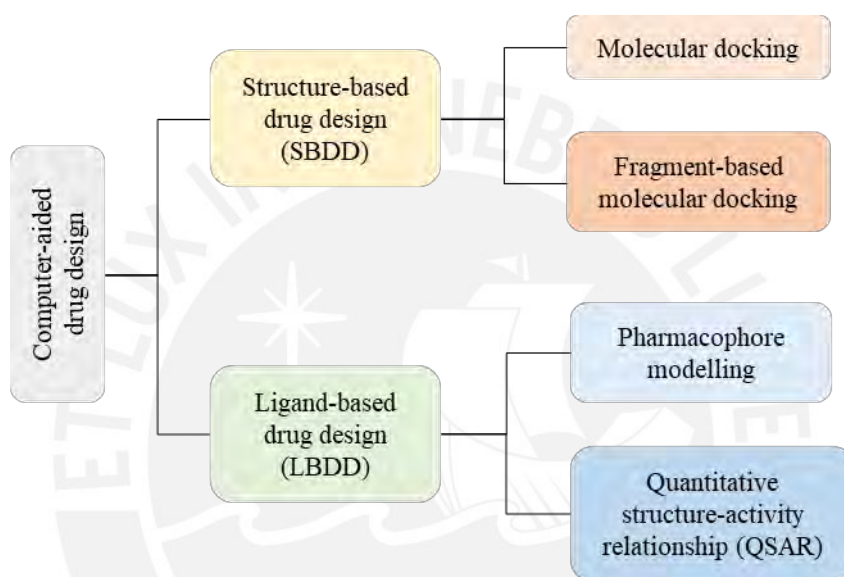
Figure 7. Classification of computer-aided drug design (CADD).

Structure-based and ligand-based drug design rely on different methods for drug development (Figure 7). Frequently used SBDD methods include molecular docking and fragment-based docking. These methods require preparation of the target which involve several steps including adding hydrogens, missing side-chains, and missing bonds to the basic skeleton; fixing chain breaks, predicting protonation states, and identifying relevant co-crystallized water molecules.[76] In addition, prior knowledge of the binding site is required.[69] This information can be retrieved from the structure of the co-crystallized protein with ligands, if available, or predicted with *in silico* methods.[69]

Molecular docking is a technique that calculates the affinity of molecules for the binding site of a target protein and predicts their conformation and orientation within this target.[69,70] Molecules can assume various conformations within the binding site of the target. To generate the various conformations, better known as poses, a molecule can assume within the binding site, the docking software uses protein-ligand sampling algorithms.[77] Then, to evaluate and rank the various poses generated, scoring functions are used which predict the binding affinity between the protein and ligand.[78]

Fragment-based drug design, on the other hand, is a method that involves the identification of small chemical fragments that weakly bind to a target protein (micro to millimolar affinity) and their optimization into lead compounds of higher affinity by means of fragment growing, merging, or linking;[79] with the aid of molecular docking. Therefore, fragment-based drug design can also be referred as fragment based docking.[69] The theoretical basis for this is that the Gibbs free energy changes which follow the binding of an A-B molecule to a protein is the sum of "intrinsic binding energies" of A and B and the "connection Gibbs energy".[80] In addition, the overall binding energy of a molecule could be estimated from the binding energies of the individual functional groups of the molecule; this calculated value is then compared to the experimental binding free energy and the closeness between these is a measure of the fit between the drug and the protein.[81] Fragments selection follow the "rule of three" which considers three physicochemical properties: molecular weight <300 g/mol, number of hydrogen bond donors and acceptors ≤3, and the calculated LogP is ≤3.[82] Since fragments have low affinity for the target, sensitive techniques are used to identify fragments, including NMR, X-ray crystallography, and surface plasmon resonance (SPR).[79]

Computationally, the chemical fragment data can be attained through molecular docking of a library of structurally diverse fragments that follow the "rule of three".[69] The difference with

molecular docking is that instead of entire molecules, fragments are docked. Affinity of these individual fragments is low but can be improved by conveniently linking them through bonds that permit binding to different protein pockets.[79]

Within ligand-based drug design, two of the main approaches include pharmacophore modelling and quantitative structure-activity relationship (QSAR).

A pharmacophore model is a set of steric and electronic features necessary for ligand recognition by the target protein and for prompting a biological response.[70,83] These models are built based on molecular descriptors such as H-bond donors, H-bond acceptors, hydrophobic groups, and ionizable groups.[84] A structurally diverse set of ligands is required, containing both active and inactive ligands; this is necessary for the model to be able to differentiate between ligands that possess or not bioactivity.[70] Then, structurally diverse active ligands, in their energetically stable conformations, are arranged and superimposed to identify similar functional groups.[69] An abstract representation is created based on the similarities; for example phenyl rings are labelled as "aromatic ring" while hydroxyl groups, or analogs becomes a "hydrogen-bond donor/acceptor".[69] After the model is validated, it can be used to screen molecular databases against these features.[83]

Quantitative structure-activity relationship (QSAR) is based on the association between structural and physicochemical properties to biological activity,[69] such that structurally similar compounds display similar bioactivity, better known as similarity-property principle.[85] Classically, QSAR is defined by linear regression models based on molecules that have the same biological activity. To build reliable QSAR models, it is necessary to obtain data of bioactive compounds (20 minimum), tested on a similar biological assay.[70,86] This set of compounds share a scaffold, but have different substituents at one or more positions. Under the similarity-property principle, these gradual changes in structure accompany gradual changes in

potency leading to linear QSAR models.[85] Beyond classical QSAR, it is possible to model relationship between more diverse chemical structures, with few or no common scaffolds, with non-linear models, requiring the use of machine learning.[85] QSAR models, after evaluation with test set molecules (molecules not used to build the model), can be used to predict the biological activity of potential drugs.[83]

3.3. Chemical structures of tentative inhibitors of *Mtb*DHFR

During the last decade, several *in silico* and *in vitro* studies have led to new sets of molecular scaffolds that could be optimized with further docking studies. These structures are shown in Table 4 together with their biological data, such as dissociation constant (K_d), half maximal inhibitory concentration (IC_{50}), and actual minimum inhibitory concentration (MIC), accordingly to the studies performed on them.

The approach that led to the discovery of SK-2b, Table 4, followed the fragment-based drug discovery. Shelke and collaborators elaborated a 20 fragment library which includes nitrogen heterocycles, xanthines, and quinazolinones, structurally similar to dihydrofolic acid but that did not contain the ubiquitous 2,4-diaminopyrimidine ring, in attempt to have a more diverse library (ubiquitous moiety for many *Mtb*DHFR inhibitors).[87] Then, ligands were optimized with Ligprep module of Schrödinger (hydrogens were completed for the ligands and optimized to their low-energy 3D conformation) and docking was performed using Glide by Schrodinger. Docking studies showed that all molecules formed hydrogen bonds with Ile94, a key residue within the binding site of *Mtb*DHFR. These molecules were synthesized for the *in vitro* studies and screened against *Mtb*DHFR and *Mtb*(H_{37}Rv) to determine the IC_{50} and MIC respectively (SK-2b, Table 4).

On the other hand, compound KC-11 was developed by Sharma and collaborators,[59,88] first through virtual screening, followed by structural modification. In their 2018 publication, they

screened merged public domain databases (NCI and drug bank database) using Lipinski rule[89] and ADME (acronym for pharmacokinetic parameters adsorption, distribution, metabolism, and excretion). Then, this set of molecules were subjected to docking using three precision options (high throughput virtual screening, standard precision, and extra precision) against MtbDHFR (PDB: 1DF7), from which 100 hits were determined. Later, the docking was repeated but against hDHFR (PDB: 1OHJ) for selectivity studies. The compounds – 50 overall – with the highest scores against MtbDHFR and lowest for hDHFR were selected. These were filtered to 10 after consensus docking using both Glide module of Maestro 9.4 and GOLD Suite 5.2.2. Consensus docking is a method that combines more than one scoring algorithm, in this case, two different programs with different algorithms, with the purpose of achieving more accurate binding affinities.[90] Only one molecule of these ten hits was synthesized for biological assays: IND-07. Later, IND-07 was functionalized to obtain KC-11, whose MIC value was of 1.56 μg/mL.[88] Its potency could be explained because of its interaction with key amino acids of MtbDHFR such as Phe31 and Gln28, observed in molecular docking studies.
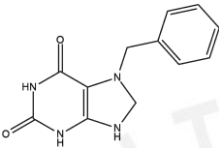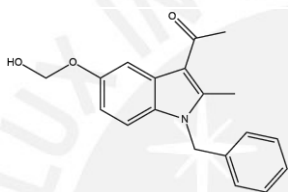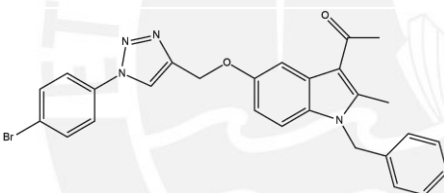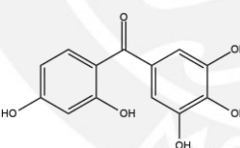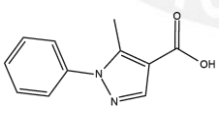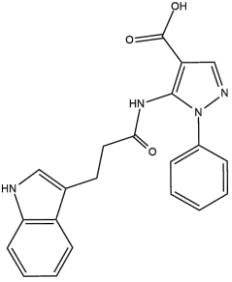
On a third report Sharma and collaborates[91] developed another inhibitor. They performed a virtual screening with 22,401 compounds from the MolMall database. These were filtered using Lipinski's rule of five and reactive functionalities. Then, for docking studies, the crystal structures (1DF7 and 1OHJ) were prepared with Maestro, while, ligands were prepared with the Ligprep module of Schrödinger-10.6. Docking against MtbDHFR was performed with the software Glide 10.6 by Schrödinger, in three steps: Glide high-throughput virtual screening (18,256 compounds), Glide standard precision (1,696 compounds), and Glide extra precision (100 compounds). These 100 compounds were then docked against hDHFR; those with the lower docking scores against hDHFR and highest scores against MtbDHFR were selected. The 16 ligands that showed the highest binding and that were available in sufficient quantities for biological studies were studied in vitro for antitubercular activity against MtbDHFR and

*h*DHFR enzymes (Table 4). In this manner, the scaffold 11436 (Table 4) was discovered which yielded excellent results compared to other inhibitors. The reason why this compound has the highest MIC and IC_{50} values may rely on the hydrogen bonding it achieves with amino acids Ile94, Gln28, Asp27, and Leu24. The last three amino acids are present at the GOL-binding site, which again, is only present in *Mtb*DHFR, explaining its selectivity. In addition, compound 11436 was capable of π stacking with amino acid Phe31.

Ribeiro and collaborators, using the fragment-based drug discovery approach, arrived to scaffold R-1d (see Table 4).[53] For this molecule, following the "rule of three",[82] *Mtb*DHFR:NADPH was screened against 1250 compounds from the Maybridge RO3 library using differential scanning fluorimetry (DSF). From this group of molecules, 37 were selected from which, 30 were rescreened but using saturation transfer difference (STD) NMR. This NMR technique is used to identify signals of the ligand-receptor complex, as well as signals of the free ligand. It does so by acquiring two ^{1}H-NMR spectra (1. on-resonance and 2. off-resonance) of a mixture of the target protein and ~100-fold moles of ligand, dissolved in pure D_2O.[92] Meanwhile, K_d values were determined using isothermal titration calorimetry (ITC). The analysis yielded 21 fragments, nine of which were co-crystalized with *Mtb*DHFR and NADPH. Fragment R-1 (see Table 4) occupied the GOL binding site of *Mtb*DHFR ($K_d =$ 641±124 μM) with the carboxylic acid hydrogen bonding to residue Gln28, which is important for selectivity over *h*DHFR. For this reason, R-1 was selected for further optimization, while keeping the aryl ring which was involved in π-interactions with Phe31. Fragments from an in-house library were linked to R-1, leading to the development of R-1d resulting in a smaller K_d. It co-crystallized with *Mtb*DHFR and NADPH. The crystal structure revealed a hydrogen bond between Gln28 and the propanamide group linker. However, interactions with the GOL binding site were lost due to R-1d adopting a different binding mode due to a stronger interaction between the indole group with Phe31 and the carboxylic acid with Arg60. Nonetheless, the

importance of this study was the identification of pyrimidine-free scaffold R-1 which, through a fragment growing approach, could maintain the GOL binding site interaction while improving K_d values.

Table 4. *In vitro* biological evaluation of potential scaffolds against *Mtb*DFHR and *Mtb*H$_{37}$Rv.

Compound	Structure	K_d (µM)	*In vitro* activity vs H$_{37}$R$_v$ (MIC in µg/mL)	*Mtb*DHFR IC$_{50}$ (µM)	Ref.
SK-2b		-	31.5	38.6	87
IND-07		-	-	150	59
KC-11		-	1.56	6.79	88
11436		-	0.167	5.50	91
R-1		641±124	-	-	53
R-1d		17±2	-	-	53

Having introduced enzyme Rv2671 and the alternative folate cycle, the work of Hajian and collaborators,[42] that led to inhibitor UCP1172 (Figure 8), is noteworthy. They identified a series of inhibitors termed ionized non-classical antifolates (INCAs), which consist of 2,4-diaminopyrimidine ring and a biaryl system linked through a propargyl bridge. These were selected from a previous study by the same research group; they biologically screened 22 propargyl-linked antifolates (these had been originally designed to inhibit DHFRs of *Staphylococcus aureus, Klebsiella pneumoniae, Candida albicans,* and *Steptococcus pyogenes*) against several strains of *Mtb*, looking for growth inhibition of the bacterium.[93] To understand the interactions between ligand and target, these molecules, together with the modified *p*-amino salicylic acid, PAS-M (Figure 8) – functionalized according to Dawadi and collaborators[94] – were co-crystallized with *Mtb*DHFR bound to NADPH. In Figure 8, the biological data of these compounds is contrasted against that of MTX. The molecule UCP1172 showed the greatest potential as an inhibitor (Figure 8). It had a similar binding mode to the one reported for MTX in *Mtb*DHFR, exhibiting hydrogen bonding with amino acids Ile5 and Ile94. In addition, it hydrogen bonds with the side chain of Asp27 from the GOL binding site and there are also π-stacking interactions with the Phe31 residue. Also, when UCP1172 was tested against *Mtb* Rv2671 it showed potent action.

MTX

MIC: >100 µg/mL
*Mtb*DHFR K_i: 1.6 ± 0.16 nM
*h*DHFR K_i: 0.7 ± 0.11 nM
Mtb Rv2671 K_i: ND

PAS-M

MIC: 8 µg/mL
MtbDHFR K_i: 750 ± 120 nM
hDHFR K_i: ND
Mtb Rv2671 K_i: $27,500 \pm 3500$ nM

UCP1172

MIC: 0.03 µg/mL
*Mtb*DHFR K_i: 0.91 ± 0.15 nM
*h*DHFR K_i: 60 ± 15 nM
Mtb Rv2671 K_i: 80 ± 6.5 nM
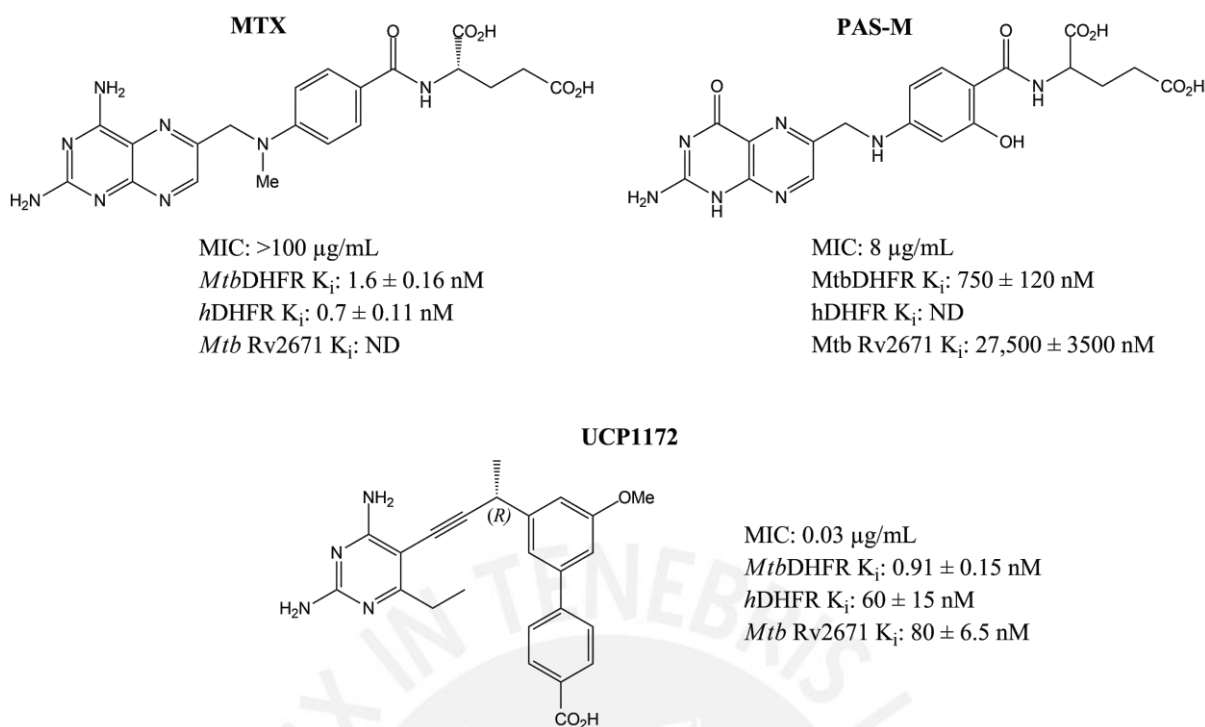
Figure 8. Biological evaluation of UCP1172, MTX, and PAS-M. (Information taken from reference 42).

4. Conclusions and perspectives

- Tuberculosis, caused by *M. tuberculosis*, is the leading cause of death globally, only behind COVID-19. The increasing number of multi and extensive drug resistant (MDR, XDR) TB requires new, more selective and less toxic therapeutic targets.

- *M. tuberculosis* dihydrofolate reductase, *Mtb*DHFR, is an enzyme involved in the folate pathway. Its inhibition is linked to the interruption of DNA synthesis and death of the bacterium. The structural differences with respect to its human counterpart, *h*DHFR, such as the absence of GOL-binding site, makes it a promising chemotherapeutic target to fight TB.

- With the improvement of computational power and the emergence of more potent algorithms, Computer-Aided Drug Design (CADD) has become the standard for drug

31

development ventures. It reduces time and costs and it allows simulations of drug-receptor interactions.

- Understanding the interactions that take place within the binding site of the inhibitor in the enzyme, facilitates the design of inhibitors with higher affinity by introducing moieties that could increase the interactions with the residues in the active site. This was the case of KC-11 from its predecessor IND-07.

- The virtual inhibitors described herein are mostly heterocycles of moderate size (<515 g/mol) of diverse functionality (pyrimidines, pyrazines, triazoles, biphenyls).

- The GOL binding site (involving residues and Trp22, Leu24, Asp27, Gln28) – absent in *h*DHFR – close to the active site of the DHF substrate (constituted by Trp6, Ala7, Asp27, Gln28, Ala29, Phe31, Arg32, Leu50, Val54, Leu54, Arg60, Ile94, Thr113) offers the unique possibility of searching for more selective inhibitors against the pathogenic DHFR.

- Understanding the details of the active site of the substrate, the co-factor and the GOL, allows the redesign of the scaffolds, with the aim of increasing the affinity for the active site and the development of potential inhibitors of *Mtb*DHFR.

- Compounds SK-2b, KC-11, 11436, initially narrowed down through virtual screening from fragment libraries and databases containing hundreds of compounds, and R-1d, and UPC1172, experimentally *in-vitro* screened, may be worth for further optimize by docking studies which simulate the enzyme-inhibitor complex interactions.

5. References

(1) Ashkar, S. R.; Rajeswaran, W.; Lee, P. H.; Yeomans, L.; Thrasher, C. M.; Franzblau, S. G.; Murakami, K. S.; Showalter, H. D.; Garcia, G. A. Optimization of Benzoxazinorifamycins to Minimize hPXR Activation for the Treatment of Tuberculosis and HIV Coinfection. *ACS Infect. Dis.* **2022**. https://doi.org/10.1021/acsinfecdis.1c00635.

(2) WHO. *Global Tuberculosis Report 2022*. World Health Organization. https://www.who.int/teams/global-tuberculosis-programme/tb-reports/global-tuberculosis-report-2022 (accessed 2022-12-01).

(3) Pezzella, A. T. History of Pulmonary Tuberculosis. *Thorac. Surg. Clin.* **2019**, *29* (1), 1–17. https://doi.org/10.1016/j.thorsurg.2018.09.002.

(4) Selgelid, M. J. Ethics, Tuberculosis and Globalization. *Public Health Ethics* **2008**, *1* (1), 10–20. https://doi.org/10.1093/phe/phn001.

(5) Lory, S. The Family Mycobacteriaceae. In *The Prokaryotes: Actinobacteria*; Rosenberg, E., DeLong, E. F., Lory, S., Stackebrandt, E., Thompson, F., Eds.; Springer: Berlin, Heidelberg, 2014; pp 571–575. https://doi.org/10.1007/978-3-642-30138-4_339.

(6) Best, M.; Sattar, S. A.; Springthorpe, V. S.; Kennedy, M. E. Efficacies of Selected Disinfectants against Mycobacterium Tuberculosis. *J. Clin. Microbiol.* **1990**, *28* (10), 2234–2239. https://doi.org/10.1128/jcm.28.10.2234-2239.1990.

(7) Bhat, Z. S.; Rather, M. A.; Maqbool, M.; Lah, H. U.; Yousuf, S. K.; Ahmad, Z. Cell Wall: A Versatile Fountain of Drug Targets in Mycobacterium Tuberculosis. *Biomed. Pharmacother.* **2017**, *95*, 1520–1534. https://doi.org/10.1016/j.biopha.2017.09.036.

(8) Hermann, C.; Karamchand, L.; Blackburn, J. M.; Soares, N. C. Cell Envelope Proteomics of Mycobacteria. *J. Proteome Res.* **2021**, *20* (1), 94–109. https://doi.org/10.1021/acs.jproteome.0c00650.

(9) Gygli, S. M.; Borrell, S.; Trauner, A.; Gagneux, S. Antimicrobial Resistance in Mycobacterium Tuberculosis: Mechanistic and Evolutionary Perspectives. *FEMS Microbiol. Rev.* **2017**, *41* (3), 354–373. https://doi.org/10.1093/femsre/fux011.

(10) Shetye, G. S.; Franzblau, S. G.; Cho, S. New Tuberculosis Drug Targets, Their Inhibitors, and Potential Therapeutic Impact. *Transl. Res.* **2020**, *220*, 68–97. https://doi.org/10.1016/j.trsl.2020.03.007.

(11) Bussi, C.; Gutierrez, M. G. Mycobacterium Tuberculosis Infection of Host Cells in Space and Time. *FEMS Microbiol. Rev.* **2019**, *43* (4), 341–361. https://doi.org/10.1093/femsre/fuz006.

(12) Natarajan, A.; Beena, P. M.; Devnikar, A. V.; Mali, S. A Systemic Review on Tuberculosis. *Indian J. Tuberc.* **2020**, *67* (3), 295–311. https://doi.org/10.1016/j.ijtb.2020.02.005.

(13) Cambier, C. J.; Falkow, S.; Ramakrishnan, L. Host Evasion and Exploitation Schemes of Mycobacterium Tuberculosis. *Cell* **2014**, *159* (7), 1497–1509. https://doi.org/10.1016/j.cell.2014.11.024.

(14)   Sia, J. K.; Rengarajan, J. Immunology of Mycobacterium Tuberculosis Infections. *Microbiol. Spectr.* **2019**, *7* (4), 7.4.6. https://doi.org/10.1128/microbiolspec.GPP3-0022-2018.

(15)   Ganchua, S. K. C.; Cadena, A. M.; Maiello, P.; Gideon, H. P.; Myers, A. J.; Junecko, B. F.; Klein, E. C.; Lin, P. L.; Mattila, J. T.; Flynn, J. L. Lymph Nodes Are Sites of Prolonged Bacterial Persistence during Mycobacterium Tuberculosis Infection in Macaques. *PLOS Pathog.* **2018**, *14* (11), e1007337. https://doi.org/10.1371/journal.ppat.1007337.

(16)   Singh, R.; Dwivedi, S. p.; Gaharwar, U. s.; Meena, R.; Rajamani, P.; Prasad, T. Recent Updates on Drug Resistance in Mycobacterium Tuberculosis. *J. Appl. Microbiol.* **2020**, *128* (6), 1547–1567. https://doi.org/10.1111/jam.14478.

(17)   Dookie, N.; Rambaran, S.; Padayatchi, N.; Mahomed, S.; Naidoo, K. Evolution of Drug Resistance in Mycobacterium Tuberculosis: A Review on the Molecular Determinants of Resistance and Implications for Personalized Care. *J. Antimicrob. Chemother.* **2018**, *73* (5), 1138–1151. https://doi.org/10.1093/jac/dkx506.

(18)   Mukonzo, J.; Aklillu, E.; Marconi, V.; Schinazi, R. F. Potential Drug–Drug Interactions between Antiretroviral Therapy and Treatment Regimens for Multi-Drug Resistant Tuberculosis: Implications for HIV Care of MDR-TB Co-Infected Individuals. *Int. J. Infect. Dis.* **2019**, *83*, 98–101. https://doi.org/10.1016/j.ijid.2019.04.009.

(19)   Perveen, S.; Kumari, D.; Singh, K.; Sharma, R. Tuberculosis Drug Discovery: Progression and Future Interventions in the Wake of Emerging Resistance. *Eur. J. Med. Chem.* **2022**, *229*, 114066. https://doi.org/10.1016/j.ejmech.2021.114066.

(20)   Aronson, J. K. *Meyler's Side Effects of Drugs: The International Encyclopedia of Adverse Drug Reactions and Interactions*, Sixteenth Edition.; Elsevier, 2016.

(21)   Combrink, M.; Loots, D. T.; du Preez, I. Metabolomics Describes Previously Unknown Toxicity Mechanisms of Isoniazid and Rifampicin. *Toxicol. Lett.* **2020**, *322*, 104–110. https://doi.org/10.1016/j.toxlet.2020.01.018.

(22)   Ramanathan, M. R.; Howell, C. K.; Sanders, J. M. Chapter 29 - Drugs in Tuberculosis and Leprosy. In *Side Effects of Drugs Annual*; Ray, S. D., Ed.; A Worldwide Yearly Survey of New Data in Adverse Drug Reactions; Elsevier, 2018; Vol. 40, pp 363–376. https://doi.org/10.1016/bs.seda.2018.06.014.

(23)   Deoghare, S. Bedaquiline: A New Drug Approved for Treatment of Multidrug-Resistant Tuberculosis. *Indian J. Pharmacol.* **2013**, *45* (5), 536. https://doi.org/10.4103/0253-7613.117765.

(24)   Schecter, G. F.; Scott, C.; True, L.; Raftery, A.; Flood, J.; Mase, S. Linezolid in the Treatment of Multidrug-Resistant Tuberculosis. *Clin. Infect. Dis.* **2010**, *50* (1), 49–55. https://doi.org/10.1086/648675.

(25)   Mirnejad, R.; Asadi, A.; Khoshnood, S.; Mirzaei, H.; Heidary, M.; Fattorini, L.; Ghodousi, A.; Darban-Sarokhalil, D. Clofazimine: A Useful Antibiotic for Drug-Resistant Tuberculosis. *Biomed. Pharmacother.* **2018**, *105*, 1353–1359. https://doi.org/10.1016/j.biopha.2018.06.023.

(26)   Tang, S.; Yao, L.; Hao, X.; Liu, Y.; Zeng, L.; Liu, G.; Li, M.; Li, F.; Wu, M.; Zhu, Y.; Sun, H.; Gu, J.; Wang, X.; Zhang, Z. Clofazimine for the Treatment of Multidrug-Resistant Tuberculosis: Prospective, Multicenter, Randomized Controlled Study in China. *Clin. Infect. Dis.* **2015**, *60* (9), 1361–1367. https://doi.org/10.1093/cid/civ027.

(27)   Rodloff, A. C.; Goldstein, E. J. C.; Torres, A. Two Decades of Imipenem Therapy. *J. Antimicrob. Chemother.* **2006**, *58* (5), 916–929. https://doi.org/10.1093/jac/dkl354.

(28)   Li, W.-J.; Li, D.-F.; Hu, Y.-L.; Zhang, X.-E.; Bi, L.-J.; Wang, D.-C. Crystal Structure of L,D-Transpeptidase LdtMt2 in Complex with Meropenem Reveals the Mechanism of Carbapenem against Mycobacterium Tuberculosis. *Cell Res.* **2013**, *23* (5), 728–731. https://doi.org/10.1038/cr.2013.53.

(29)   Zhanel, G. G.; Wiebe, R.; Dilay, L.; Thomson, K.; Rubinstein, E.; Hoban, D. J.; Noreddin, A. M.; Karlowsky, J. A. Comparative Review of the Carbapenems. *Drugs* **2007**, *67* (7), 1027–1052. https://doi.org/10.2165/00003495-200767070-00006.

(30)   Arnold, A.; Cooke, G. S.; Kon, O. M.; Dedicoat, M.; Lipman, M.; Loyse, A.; Chis Ster, I.; Harrison, T. S. Adverse Effects and Choice between the Injectable Agents Amikacin and Capreomycin in Multidrug-Resistant Tuberculosis. *Antimicrob. Agents Chemother.* **2017**, *61* (9), e02586-16. https://doi.org/10.1128/AAC.02586-16.

(31)   Magnet, S.; Blanchard, J. S. Molecular Insights into Aminoglycoside Action and Resistance. *Chem. Rev.* **2005**, *105* (2), 477–498. https://doi.org/10.1021/cr0301088.

(32)   Carter, A. P.; Clemons, W. M.; Brodersen, D. E.; Morgan-Warren, R. J.; Wimberly, B. T.; Ramakrishnan, V. Functional Insights from the Structure of the 30S Ribosomal Subunit and Its Interactions with Antibiotics. *Nature* **2000**, *407* (6802), 340–348. https://doi.org/10.1038/35030019.

(33)   Weekes, C.; Kotra, L. P. Mycobacterium Tuberculosis Infections. In *xPharm: The Comprehensive Pharmacology Reference*; Enna, S. J., Bylund, D. B., Eds.; Elsevier: New York, 2007; pp 1–7. https://doi.org/10.1016/B978-008055232-3.60889-X.

(34)   Vilchèze, C.; Weisbrod, T. R.; Chen, B.; Kremer, L.; Hazbón, M. H.; Wang, F.; Alland, D.; Sacchettini, J. C.; Jacobs, W. R. Altered NADH/NAD+ Ratio Mediates Coresistance to Isoniazid and Ethionamide in Mycobacteria. *Antimicrob. Agents Chemother.* **2005**, *49* (2), 708–720. https://doi.org/10.1128/AAC.49.2.708-720.2005.

(35)   Wang, F.; Langley, R.; Gulten, G.; Dover, L. G.; Besra, G. S.; Jacobs, W. R., Jr.; Sacchettini, J. C. Mechanism of Thioamide Drug Action against Tuberculosis and Leprosy. *J. Exp. Med.* **2007**, *204* (1), 73–78. https://doi.org/10.1084/jem.20062100.

(36)   Tiberi, S.; Muñoz-Torrico, M.; Duarte, R.; Dalcolmo, M.; D'Ambrosio, L.; Migliori, G.-B. New Drugs and Perspectives for New Anti-Tuberculosis Regimens. *Pulmonology* **2018**, *24* (2), 86–98. https://doi.org/10.1016/j.rppnen.2017.10.009.

(37)   Brucoli, F.; D McHugh, T. Rifamycins: Do Not Throw the Baby out with the Bathwater. Is Rifampicin Still an Effective Anti-Tuberculosis Drug? *Future Med. Chem.* **2021**, *13* (24), 2129–2131. https://doi.org/10.4155/fmc-2021-0249.

(38)   Cao, J.; Mi, Y.; Shi, C.; Bian, Y.; Huang, C.; Ye, Z.; Liu, L.; Miao, L. First-Line Anti-Tuberculosis Drugs Induce Hepatotoxicity: A Novel Mechanism Based on a Urinary Metabolomics Platform. *Biochem. Biophys. Res. Commun.* **2018**, *497* (2), 485–491. https://doi.org/10.1016/j.bbrc.2018.02.030.

(39)   WHO. *WHO consolidated guidelines on tuberculosis: module 4: treatment: drug-resistant tuberculosis treatment*. World Health Organization. https://www.who.int/publications-detail-redirect/9789240007048 (accessed 2022-10-15).

(40)   WHO. *WHO operational handbook on tuberculosis: module 4: treatment: drug-resistant tuberculosis treatment*. World Health Organization. https://www.who.int/publications-detail-redirect/9789240006997 (accessed 2022-10-15).

(41)   Prasad, R.; Singh, A.; Gupta, N. Adverse Drug Reactions with First-Line and Second-Line Drugs in Treatment of Tuberculosis. *Ann. Natl. Acad. Med. Sci. India* **2021**, *57* (1), 15–35. https://doi.org/10.1055/s-0040-1722535.

(42)   Hajian, B.; Scocchera, E.; Shoen, C.; Krucinska, J.; Viswanathan, K.; G-Dayanandan, N.; Erlandsen, H.; Estrada, A.; Mikušová, K.; Korduláková, J.; Cynamon, M.; Wright, D. Drugging the Folate Pathway in Mycobacterium Tuberculosis: The Role of Multi-Targeting Agents. *Cell Chem. Biol.* **2019**, *26* (6), 781-791.e6. https://doi.org/10.1016/j.chembiol.2019.02.013.

(43)   Bertacine Dias, M. V.; Santos, J. C.; Libreros-Zúñiga, G. A.; Ribeiro, J. A.; Chavez-Pacheco, S. M. Folate Biosynthesis Pathway: Mechanisms and Insights into Drug Design for Infectious Diseases. *Future Med. Chem.* **2018**, *10* (8), 935–959. https://doi.org/10.4155/fmc-2017-0168.

(44)   Froese, D. S.; Fowler, B.; Baumgartner, M. R. Vitamin B12, Folate, and the Methionine Remethylation Cycle—Biochemistry, Pathways, and Regulation. *J. Inherit. Metab. Dis.* **2019**, *42* (4), 673–685. https://doi.org/10.1002/jimd.12009.

(45)   Then, R. Bacterial Dihydrofolate Reductase*. In *xPharm: The Comprehensive Pharmacology Reference*; Enna, S. J., Bylund, D. B., Eds.; Elsevier: New York, 2007; pp 1–6. https://doi.org/10.1016/B978-008055232-3.60502-1.

(46)   Zarou, M. M.; Vazquez, A.; Vignir Helgason, G. Folate Metabolism: A Re-Emerging Therapeutic Target in Haematological Cancers. *Leukemia* **2021**, *35* (6), 1539–1551. https://doi.org/10.1038/s41375-021-01189-2.

(47)   Ducker, G. S.; Rabinowitz, J. D. One-Carbon Metabolism in Health and Disease. *Cell Metab.* **2017**, *25* (1), 27–42. https://doi.org/10.1016/j.cmet.2016.08.009.

(48)   Li, R.; Sirawaraporn, R.; Chitnumsub, P.; Sirawaraporn, W.; Wooden, J.; Athappilly, F.; Turley, S.; Hol, W. G. Three-Dimensional Structure of M. Tuberculosis Dihydrofolate Reductase Reveals Opportunities for the Design of Novel Tuberculosis Drugs. *J. Mol. Biol.* **2000**, *295* (2), 307–323. https://doi.org/10.1006/jmbi.1999.3328.

(49)   RCSB Protein Data Bank. *3D Protein Feature View: 6NND*. RCSB PDB. https://www.rcsb.org/3d-sequence/6NND?assemblyId=1 (accessed 2022-11-30).

(50)   RCSB Protein Data Bank. *3D Protein Feature View: 1DG8*. RCSB PDB. https://www.rcsb.org/3d-sequence/1DG8?assemblyId=1 (accessed 2022-11-30).

(51)   RCSB Protein Data Bank. *3D Protein Feature View: 1DF7*. RCSB PDB. https://www.rcsb.org/3d-sequence/1DF7?assemblyId=1 (accessed 2022-11-30).

(52)   Ribeiro, J. A.; Chavez-Pacheco, S. M.; de Oliveira, G. S.; Silva, C. S.; Giudice, J. H. P.; Libreros-Zúñiga, G. A.; Dias, M. V. B. Crystal Structures of the Closed Form of Mycobacterium Tuberculosis Dihydrofolate Reductase in Complex with Dihydrofolate and Antifolates. *Acta Crystallogr. Sect. Struct. Biol.* **2019**, *75* (7), 682–693. https://doi.org/10.1107/S205979831900901X.

(53)   Ribeiro, J. A.; Hammer, A.; Libreros-Zúñiga, G. A.; Chavez-Pacheco, S. M.; Tyrakis, P.; de Oliveira, G. S.; Kirkman, T.; El Bakali, J.; Rocco, S. A.; Sforça, M. L.; Parise-Filho, R.; Coyne, A. G.; Blundell, T. L.; Abell, C.; Dias, M. V. B. Using a Fragment-Based Approach to Identify Alternative Chemical Scaffolds Targeting Dihydrofolate Reductase from Mycobacterium Tuberculosis. *ACS Infect. Dis.* **2020**, *6* (8), 2192–2201. https://doi.org/10.1021/acsinfecdis.0c00263.

(54)   Nixon, M. R.; Saionz, K. W.; Koo, M.-S.; Szymonifka, M. J.; Jung, H.; Roberts, J. P.; Nandakumar, M.; Kumar, A.; Liao, R.; Rustad, T.; Sacchettini, J. C.; Rhee, K. Y.; Freundlich, J. S.; Sherman, D. R. Folate Pathway Disruption Leads to Critical Disruption of Methionine Derivatives in Mycobacterium Tuberculosis. *Chem. Biol.* **2014**, *21* (7), 819–830. https://doi.org/10.1016/j.chembiol.2014.04.009.

(55)   Kumar, A.; Zhang, M.; Zhu, L.; Liao, R. P.; Mutai, C.; Hafsat, S.; Sherman, D. R.; Wang, M.-W. High-Throughput Screening and Sensitized Bacteria Identify an M. Tuberculosis Dihydrofolate Reductase Inhibitor with Whole Cell Activity. *PLOS ONE* **2012**, *7* (6), e39961. https://doi.org/10.1371/journal.pone.0039961.

(56)   Kronenberger, T.; Ferreira, G. M.; de Souza, A. D. F.; da Silva Santos, S.; Poso, A.; Ribeiro, J. A.; Tavares, M. T.; Pavan, F. R.; Trossini, G. H. G.; Dias, M. V. B.; Parise-Filho, R. Design, Synthesis and Biological Activity of Novel Substituted 3-Benzoic Acid Derivatives as MtDHFR Inhibitors. *Bioorg. Med. Chem.* **2020**, *28* (15), 115600. https://doi.org/10.1016/j.bmc.2020.115600.

(57)   El-Hamamsy, M. H.; Smith, A.; Thompson, A.; Threadgill, M. Structure-Based Design, Synthesis and Preliminary Evaluation of Selective Inhibitors of Dihydrofolate Reductase from Mycobacterium Tuberculosis. *Bioorg. Med. Chem.* **2007**. https://doi.org/10.1016/J.BMC.2007.04.011.

(58)   Hong, W.; Wang, Y.; Chang, Z.; Yang, Y.; Pu, J.; Sun, T.; Kaur, S.; Sacchettini, J. C.; Jung, H.; Lin Wong, W.; Fah Yap, L.; Fong Ngeow, Y.; Paterson, I. C.; Wang, H. The Identification of Novel Mycobacterium Tuberculosis DHFR Inhibitors and the Investigation of Their Binding Preferences by Using Molecular Modelling. *Sci. Rep.* **2015**, *5* (1), 15328. https://doi.org/10.1038/srep15328.

(59)   Sharma, K.; Tanwar, O.; Sharma, S.; Ali, S.; Alam, M. M.; Zaman, M. S.; Akhter, M. Structural Comparison of Mtb-DHFR and h-DHFR for Design, Synthesis and Evaluation of Selective Non-Pteridine Analogues as Antitubercular Agents. *Bioorganic Chem.* **2018**, *80*, 319–333. https://doi.org/10.1016/j.bioorg.2018.04.022.

(60)   Cheng, Y.-S.; Sacchettini, J. C. Structural Insights into Mycobacterium Tuberculosis Rv2671 Protein as a Dihydrofolate Reductase Functional Analogue Contributing to Para-Aminosalicylic Acid Resistance. *Biochemistry* **2016**, *55* (7), 1107–1119. https://doi.org/10.1021/acs.biochem.5b00993.

(61)   Gullapalli, S. Drug Target Identification and Validation. In *Drug Discovery and Development: From Targets and Molecules to Medicines*; Poduri, R., Ed.; Springer: Singapore, 2021; pp 235–249. https://doi.org/10.1007/978-981-15-5534-3_8.

(62)   Deshaies, R. J. Multispecific Drugs Herald a New Era of Biopharmaceutical Innovation. *Nature* **2020**, *580* (7803), 329–338. https://doi.org/10.1038/s41586-020-2168-1.

(63)   Wagner, B. K. The Resurgence of Phenotypic Screening in Drug Discovery and Development. *Expert Opin. Drug Discov.* **2016**, *11* (2), 121–125. https://doi.org/10.1517/17460441.2016.1122589.

(64)   Moffat, J. G.; Vincent, F.; Lee, J. A.; Eder, J.; Prunotto, M. Opportunities and Challenges in Phenotypic Drug Discovery: An Industry Perspective. *Nat. Rev. Drug Discov.* **2017**, *16* (8), 531–543. https://doi.org/10.1038/nrd.2017.111.

(65)   Zheng, W.; Thorne, N.; McKew, J. C. Phenotypic Screens as a Renewed Approach for Drug Discovery. *Drug Discov. Today* **2013**, *18* (21), 1067–1073. https://doi.org/10.1016/j.drudis.2013.07.001.

(66)   de Oliveira, A. M.; Rudrapal, M. Chapter 1 - Introduction to Drug Design and Discovery. In *Computer Aided Drug Design (CADD): From Ligand-Based Methods to Structure-Based Approaches*; Rudrapal, M., Egbuna, C., Eds.; Drug Discovery Update; Elsevier, 2022; pp 1–15. https://doi.org/10.1016/B978-0-323-90608-1.00008-3.

(67)   Wouters, O. J.; McKee, M.; Luyten, J. Estimated Research and Development Investment Needed to Bring a New Medicine to Market, 2009-2018. *JAMA* **2020**, *323* (9), 844–853. https://doi.org/10.1001/jama.2020.1166.

(68)   Yasuo, N.; Ishida, T.; Sekijima, M. Computer Aided Drug Discovery Review for Infectious Diseases with Case Study of Anti-Chagas Project. *Parasitol. Int.* **2021**, *83*, 102366. https://doi.org/10.1016/j.parint.2021.102366.

(69)   Shaker, B.; Ahmad, S.; Lee, J.; Jung, C.; Na, D. In Silico Methods and Tools for Drug Discovery. *Comput. Biol. Med.* **2021**, *137*, 104851. https://doi.org/10.1016/j.compbiomed.2021.104851.

(70)   Vemula, D.; Jayasurya, P.; Sushmitha, V.; Kumar, Y. N.; Bhandari, V. CADD, AI and ML in Drug Discovery: A Comprehensive Review. *Eur. J. Pharm. Sci.* **2023**, *181*, 106324. https://doi.org/10.1016/j.ejps.2022.106324.

(71)   Ebhohimen, I. E.; Edemhanria, L.; Awojide, S.; Onyijen, O. H.; Anywar, G. Chapter 3 - Advances in Computer-Aided Drug Discovery. In *Phytochemicals as Lead Compounds for New Drug Discovery*; Egbuna, C., Kumar, S., Ifemeje, J. C., Ezzat, S. M., Kaliyaperumal, S., Eds.; Elsevier, 2020; pp 25–37. https://doi.org/10.1016/B978-0-12-817890-4.00003-2.

(72)   Anwar, T.; Kumar, P.; Khan, A. U. Chapter 1 - Modern Tools and Techniques in Computer-Aided Drug Design. In *Molecular Docking for Computer-Aided Drug Design*; Coumar, M. S., Ed.; Academic Press, 2021; pp 1–30. https://doi.org/10.1016/B978-0-12-822312-3.00011-4.

(73)   Lee, J.; Freddolino, P. L.; Zhang, Y. Ab Initio Protein Structure Prediction. In *From Protein Structure to Function with Bioinformatics*; J. Rigden, D., Ed.; Springer Netherlands: Dordrecht, 2017; pp 3–35. https://doi.org/10.1007/978-94-024-1069-3_1.

(74)   Kaushik, A. C.; Kumar, A.; Bharadwaj, S.; Chaudhary, R.; Sahi, S. Ligand-Based Approach for In-Silico Drug Designing. In *Bioinformatics Techniques for Drug Discovery: Applications for Complex Diseases*; Kaushik, A. C., Kumar, A., Bharadwaj, S., Chaudhary, R., Sahi, S., Eds.; SpringerBriefs in Computer Science; Springer International Publishing: Cham, 2018; pp 11–19. https://doi.org/10.1007/978-3-319-75732-2_2.

(75)   Martin, Y. C.; Kofron, J. L.; Traphagen, L. M. Do Structurally Similar Molecules Have Similar Biological Activity? *J. Med. Chem.* **2002**, *45* (19), 4350–4358. https://doi.org/10.1021/jm020155c.

(76)   Berry, M.; Fielding, B.; Gamieldien, J. Chapter 27 - Practical Considerations in Virtual Screening and Molecular Docking. In *Emerging Trends in Computational Biology, Bioinformatics, and Systems Biology*; Tran, Q. N., Arabnia, H., Eds.; Emerging Trends in Computer Science and Applied Computing; Morgan Kaufmann: Boston, 2015; pp 487–502. https://doi.org/10.1016/B978-0-12-802508-6.00027-2.

(77)   Elokely, K. M.; Doerksen, R. J. Docking Challenge: Protein Sampling and Molecular Docking Performance. *J. Chem. Inf. Model.* **2013**, *53* (8), 1934–1945. https://doi.org/10.1021/ci400040d.

(78)   Huang, S.-Y.; Grinter, S. Z.; Zou, X. Scoring Functions and Their Evaluation Methods for Protein–Ligand Docking: Recent Advances and Future Directions. *Phys. Chem. Chem. Phys.* **2010**, *12* (40), 12899–12908. https://doi.org/10.1039/C0CP00151A.

(79)   Bancet, A.; Raingeval, C.; Lomberget, T.; Le Borgne, M.; Guichou, J.-F.; Krimm, I. Fragment Linking Strategies for Structure-Based Drug Design. *J. Med. Chem.* **2020**, *63* (20), 11420–11435. https://doi.org/10.1021/acs.jmedchem.0c00242.

(80)   Jencks, W. P. On the Attribution and Additivity of Binding Energies. *Proc. Natl. Acad. Sci.* **1981**, *78* (7), 4046–4050. https://doi.org/10.1073/pnas.78.7.4046.

(81)   Andrews, P. R.; Craik, D. J.; Martin, J. L. Functional Group Contributions to Drug-Receptor Interactions. *J. Med. Chem.* **1984**, *27* (12), 1648–1657. https://doi.org/10.1021/jm00378a021.

(82)   Congreve, M.; Carr, R.; Murray, C.; Jhoti, H. A 'Rule of Three' for Fragment-Based Lead Discovery? *Drug Discov. Today* **2003**, *8* (19), 876–877. https://doi.org/10.1016/S1359-6446(03)02831-9.

(83)   Sharma, V.; Wakode, S.; Kumar, H. Chapter 2 - Structure- and Ligand-Based Drug Design: Concepts, Approaches, and Challenges. In *Chemoinformatics and Bioinformatics in the Pharmaceutical Sciences*; Sharma, N., Ojha, H., Raghav, P. K., Goyal, R. k., Eds.; Academic Press, 2021; pp 27–53. https://doi.org/10.1016/B978-0-12-821748-1.00004-X.

(84)   Kapetanovic, I. M. Computer-Aided Drug Discovery and Development (CADDD): In Silico-Chemico-Biological Approach. *Chem. Biol. Interact.* **2008**, *171* (2), 165–176. https://doi.org/10.1016/j.cbi.2006.12.006.

(85)   Muratov, E. N.; Bajorath, J.; Sheridan, R. P.; Tetko, I. V.; Filimonov, D.; Poroikov, V.; Oprea, T. I.; Baskin, I. I.; Varnek, A.; Roitberg, A.; Isayev, O.; Curtalolo, S.; Fourches, D.; Cohen, Y.; Aspuru-Guzik, A.; Winkler, D. A.; Agrafiotis, D.; Cherkasov, A.; Tropsha, A. QSAR without Borders. *Chem. Soc. Rev.* **2020**, *49* (11), 3525–3564. https://doi.org/10.1039/D0CS00098A.

(86)   Macalino, S. J. Y.; Gosu, V.; Hong, S.; Choi, S. Role of Computer-Aided Drug Design in Modern Drug Discovery. *Arch. Pharm. Res.* **2015**, *38* (9), 1686–1701. https://doi.org/10.1007/s12272-015-0640-5.

(87)   Shelke, R. U.; Degani, M. S.; Raju, A.; Ray, M. K.; Rajan, M. G. R. Fragment Discovery for the Design of Nitrogen Heterocycles as Mycobacterium Tuberculosis Dihydrofolate Reductase Inhibitors. *Arch. Pharm. (Weinheim)* **2016**, *349* (8), 602–613. https://doi.org/10.1002/ardp.201600066.

(88)   Sharma, K.; Tanwar, O.; Deora, G. S.; Ali, S.; Alam, M. M.; Zaman, M. S.; Krishna, V. S.; Sriram, D.; Akhter, M. Expansion of a Novel Lead Targeting M. Tuberculosis DHFR as Antitubercular Agents. *Bioorg. Med. Chem.* **2019**, *27* (7), 1421–1429. https://doi.org/10.1016/j.bmc.2019.02.053.

(89)   Lipinski, C. A. Lead- and Drug-like Compounds: The Rule-of-Five Revolution. *Drug Discov. Today Technol.* **2004**, *1* (4), 337–341. https://doi.org/10.1016/j.ddtec.2004.11.007.

(90)   Houston, D. R.; Walkinshaw, M. D. Consensus Docking: Improving the Reliability of Docking in a Virtual Screening Context. *J. Chem. Inf. Model.* **2013**, *53* (2), 384–390. https://doi.org/10.1021/ci300399w.

(91)   Sharma, K.; Neshat, N.; Sharma, S.; Giri, N.; Srivastava, A.; Almalki, F.; Saifullah, K.; Alam, Md. M.; Shaquiquzzaman, M.; Akhter, M. Identification of Novel Selective Mtb-DHFR Inhibitors as Antitubercular Agents through Structure-Based Computational Techniques. *Arch. Pharm. (Weinheim)* **2020**, *353* (2), 1900287. https://doi.org/10.1002/ardp.201900287.

(92)   Bhunia, A.; Bhattacharjya, S.; Chatterjee, S. Applications of Saturation Transfer Difference NMR in Biological Systems. *Drug Discov. Today* **2012**, *17* (9), 505–513. https://doi.org/10.1016/j.drudis.2011.12.016.

(93)   Hajian, B.; Scocchera, E.; Keshipeddy, S.; G-Dayanandan, N.; Shoen, C.; Krucinska, J.; Reeve, S.; Cynamon, M.; Anderson, A. C.; Wright, D. L. Propargyl-Linked Antifolates Are Potent Inhibitors of Drug-Sensitive and Drug-Resistant Mycobacterium Tuberculosis. *PLOS ONE* **2016**, *11* (8), e0161740. https://doi.org/10.1371/journal.pone.0161740.

(94)   Dawadi, S.; Kordus, S. L.; Baughn, A. D.; Aldrich, C. C. Synthesis and Analysis of Bacterial Folate Metabolism Intermediates and Antifolates. *Org. Lett.* **2017**, *19* (19), 5220–5223. https://doi.org/10.1021/acs.orglett.7b02487.